



# A Techno-Economic Analysis of Space-Based Solar Power Systems

Benedikt Kruft

*Technische Universität München*

## Abstract

Space-based solar power (SBSP) promises to provide flexible renewable baseload power. However, no full-system prototype exists due to a perceived lack of economic viability. The goal of this thesis is therefore to determine how different technology approaches can improve key technical metrics of SBSP and consequently the economics. For this purpose, we divide the system into its three main segments and define critical metrics for the performance of each subsystem. Based on these, novel technology approaches from the literature are then evaluated. For the solar satellite, we are able to show that a number of technology options exist that might improve power levels, radiation resistance, and mass-related ratios. These advances would greatly benefit overall system economics, as the space segment constitutes a big lever for enhancing the levelised cost of electricity (LCOE). Furthermore, microwave power beaming efficiencies in line with required levels have been demonstrated but so far lack the scale and distance necessary for SBSP. Ultimately, the global capacity in space lift capabilities appears to be a major bottleneck. Consequently, a reduction in mass of the satellite would not only be a matter of economics but might render any such project even possible in the first place.

*Keywords:* Energy; Solar; Space; Microwaves; Sustainability.

## 1. Introduction

The goal of this thesis is the techno-economic analysis of a general space-based solar power (SBSP) system and its subsystems. We do not focus on one of the many proposed designs in particular, but rather use a selection of the most advanced ones as a point of reference to potentially identify universal levers for progress. So far, the literature has mostly focussed on determining the general theoretical feasibility of SBSP and that of specific concepts in their entirety, such as the CASSIOPeiA project. As a result, we observed a lack in granularity that would enable the evaluation of segment-specific technology approaches. The reason for this might be the prevailing perception of SBSP as a niche and moonshot energy solution. Therefore, a targeted analysis that aims to compare technological solutions to problems specific to SBSP based on the critical metrics of each subsegment is so far

missing. Consequently, our research question is how different technology approaches can improve technical metrics of SBSP subsystems and in turn help overall system economics.

To achieve this, we start by briefly describing the context of the global energy transition and which role SBSP could play. Here we illustrate the basic idea behind SBSP plus some of the key benefits the technology has to offer. However, a comparison with other renewable generation capacities is outside the scope of this thesis. Next, we describe the concept of SBSP in more detail, including some of the most relevant modern designs under development. We then establish a general model of a SBSP system and divide it into three subsystems for further differentiation.

The division into space segment, wireless power transmission (WPT) and ground structure, as well as space launch and infrastructure then serves as the structure for our techno-economic analysis. For each of these segments, we start by identifying the metrics most critical to the technical and economic performance of the respective subsystem. This is followed by an evaluation of different technology options and developments for all subsystems by these metrics. Particularly for the space segment, each technological alternative

I want to thank the Entrepreneurial Masterclass program by UnternehmerTUM that gave me the opportunity to write about this topic and all participants who provided me with sparring opportunities and guidance. Furthermore, I want to thank Prof. Dr. Thomas Hamacher for supervising my thesis. Lastly, I am grateful for the proof-reading support provided by my family and friends.

poses a potential solution to one or multiple problems encountered during SBSP development. The selection of analysed alternatives should not be considered as exhaustive, but rather focusses on innovations that appear to be the most promising and impactful for SBSP. When discussing WPT, we will also emphasise some of the historical developments and demonstrations that have led to where the technology stands today. For the third and last segment, we will focus on the launch infrastructure in particular and only briefly discuss some production-related aspects. The three segments are concluded by a respective overview of the established alternatives or developments and an outlook on which technology combinations appear to be the most promising.

To establish equality for the comparisons of metrics drawn from the literature, some had to be recalculated or adjusted based on the disclosed data. To ensure metrics are adjusted following shared rules, we establish a common set of formulas as well as adjustment factors which are applied equally. Overall, the resulting metrics for different subsystem configurations should be seen as a heuristic approach to achieve the aforementioned comparability of different technology options. Therefore, they should be interpreted as an indicator for the order of magnitude of the impact of these technology options. All calculations are performed in a separate model, which is available upon request.

Throughout this thesis, we will also sometimes refer to some of the analyses from the literature on levelised cost of electricity (LCOE). Given how incomparable many of the absolute numbers are due to being based on sometimes vastly differing assumptions, we mostly use any breakdowns regarding cost contributions by the subsystems as a relative point of reference. This allows us to more accurately estimate how big the economic impact of the previously discussed technological levers could be, relative to each other. Consequently, this thesis does not conduct in-depth cost modelling or calculations of its own. Policy, geopolitical, and social considerations, which could impact LCOE, are also outside the scope of this thesis. It is furthermore not the purpose of this thesis to compare LCOE numbers between different renewable technologies and SBSP.

We will also introduce sustainability-related metrics such as emissions per kWh and energy payback times in the last chapter. However, a full environmental analysis of SBSP is outside the scope of this thesis. Instead, our goal is to gain a first understanding of the direction in which current approaches are trending in terms of environmental impacts and energy use. These insights can then serve as the basis for further research.

Finally, we sum up our findings, including projected LCOE numbers on a system level, and their consequences for the development of commercial SBSP systems going forward.

### 1.1. Space-based solar power for the global energy transition

The most recent IPCC report has once again made clear that quick and far-reaching action is needed if we are to have a chance at limiting global warming to 1.5 degrees (IPCC,

2022). To achieve global net zero by 2050, widespread electrification is a crucial step as it allows us to decarbonise many industries at once by turning our electricity generation green.

So far, a selection of renewable energy sources has been accessed through large amounts of investment. Solar energy has even become the cheapest energy source in history (IEA, 2020). Nonetheless, more financing is needed to overcome some of the remaining issues of our primary green energy sources, terrestrial solar and wind. Both of them suffer from intermittency, be it due to weather or day-night cycles. Furthermore, their generation is inflexible and difficult to predict far in advance. These are some of the reasons why they are generally labelled as non-dispatchable.

Space-based solar power (SBSP) promises to overcome this issue by becoming the first dispatchable renewable baseload power. The general idea is to place a satellite with extensive solar power capacity in orbit around earth. The sometimes with the help of additional mirrors and reflectors collected solar radiation is then turned into DC power before being converted to either a laser or radio frequency (RF) beam. This beam is then targeted at a receiving station on the ground, where the wirelessly transmitted power is reconverted first to DC then AC before being fed into the grid. A simplified representation of this process including efficiencies is provided in figure 1.

SBSP has a number of benefits, which are described at length in various publications (e.g. Jaffe, 2020). First, if a geostationary orbit (GEO) is chosen and the right array structure employed, the satellite would enjoy virtually constant illumination, except for during the spring and autumn equinox with a 70 min blackout each (Way & Lamyman, 2020). Hence, intermittency would no longer be an issue and the electricity generated by SBSP would be highly predictable far in advance. Second, the solar irradiation collected by the satellite would be unattenuated by weather or the atmosphere, giving a greater yield per unit surface area. Third, the beam would have to be steerable to enable precise pointing, which in turn allows flexibility in regards to where the energy is directed to. Multiple ground stations could be employed across different countries and even continents, which would then be fed by the same satellite or constellation of satellites in an alternating or semi-continuous fashion. Therefore, SBSP can also be used as a diplomatic or development tool. With mobile receiver stations, the beam could even be utilized to provide electricity to disaster-struck areas. Lastly, the technology promises to be sustainable over its lifetime, although more detailed studies will be necessary to confirm the precise extent. Overall, SBSP thus has the potential of providing semi-globally dispatchable renewable baseload power.

On the other hand, there are also some concerns associated with SBSP. Space is a domain that is difficult to control and therefore placing an asset critical to a nation's energy autonomy so far away from it comes with security concerns. Recent acts by Russia have added to this worry by showing that targeted destruction of satellites is well within the means of space-faring nations (The Economist, 2021b).

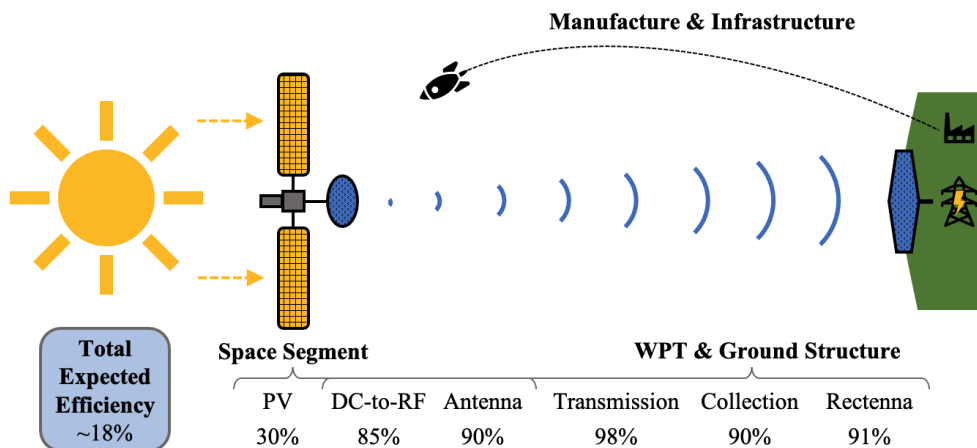


**Figure 1:** A general SBSP system generates solar power in space via a satellite which is then transformed and transmitted wirelessly, here in the form of microwaves, to a receiving station on the ground. The space segment would be manufactured on earth to be launched to and assembled in GTO. Overall, system efficiencies of 18% are expected, based on subsystem demonstrations. Own representation with efficiencies based on Jaffe (2020).

Furthermore, while reaching our climate targets requires fast and decisive action, SBSP is still not close to having any full-system prototype in orbit, thus putting in question whether it can be deployed fast enough to contribute meaningfully. Potentially, the considerable amount of funds required should then better be spent elsewhere. While the overall economics of solar power from space do appear to be competitive based on modelling (e.g. Madonna, 2018), those too would have to be confirmed in practice. Additionally, as we continue to launch ever more satellites, critical orbits such as GEO are starting to become congested (Euroconsult, 2021). Lastly, public acceptance and safety concerns around what are essentially kilometre-wide invisible energy beams will have to be addressed very early in the process.

The idea of SBSP was first described in Isaac Asimov's short story 'Reason' in 1941 and later introduced to academia by Peter Glaser (Glaser, 1968), who also filed the first SBSP patent (Glaser, 1973). What followed were a number of studies (e.g. Koomanoff, 1981) and critiques (e.g. Corson et al., 1981) of the concept. Particularly NASA and other U.S. government agencies investigated the idea in more depth, developing the two suntower concepts at 2.45 GHz (NASA, 1978) and 5.8 GHz (Davis, 2012), which are still sometimes used as reference systems. The private sector is also involved with a number of patents and plans for commercialization (Solaren, 2022).

## 1.2. Modern SBSP concepts

Today, there are a number of nations and organisations active in SBSP research and development. While for some actors, such as China, the primary goal is to develop a fully functioning concept, others focus more on advancing key technologies like WPT. For instance, Japan and the California Institute of Technology rather fall in the second category. SBSP satellites remain an ambitious idea, given that the most

advanced modern space segment designs are measured in kilometres and weigh thousands of tons. In comparison, as the largest man-made structure in space and the result of a collaboration involving space agencies from 15 countries, the ISS is barely 100 m long and weighs just over 400 t (Garcia, 2021).

Today, a variety of concepts exist that have entered advanced planning stages. The ones we have chosen as reference systems during our comparative analyses were selected based on how established they are in the literature and the quantity as well as quality of data available to perform the necessary calculations. Furthermore, we have selected space segment architectures that are different from each other to capture the impact of design variations on the critical metrics. Lastly, all of the chosen concepts have some form of government backing, which will likely be essential given the scale and ambition of SBSP. Therefore, we want to highlight the following projects, whose respective unique space segment architecture is also displayed in figure 2.

### SPS-ALPHA:

The Solar Power Satellite with Arbitrarily Large PHased Array (SPS-ALPHA) is a concept that has been developed by John Mankins since the 1990s in collaboration with NASA (Mankins, 1997). The about 4-km tall structure is comprised of an energy conversion array, which is connected to a single large reflector array via boom structures (Mankins, 2021). Once placed in GEO, it would maintain an orientation where the antenna side of the conversion array is continuously pointed at the receiving station on earth, transmitting the energy in form of microwaves at 2.45 GHz. During local night, the reflector array will redirect and concentrate the sunlight onto the photovoltaic (PV) surface to ensure continuous operation. At 7,600 t in-space mass, it is one of the heavier concepts. It is designed to deliver 2 GW of DC power to the grid

around the clock.

#### *CASSIOPeiA:*

The Constant Aperture, Solid-State, Integrated, Orbital Phased Array (CASSIOPeiA) concept has been developed by Ian Cash from International Electric. Its key feature is a 1.7-km long helical energy generation and transmission array with two conical solid-state symmetrical concentrators on either end (Cash, 2019). These primary reflectors collect, concentrate, and collimate the sunlight onto the patented helix array, which includes further concentration on the PV chips. L-shaped sandwich modules are employed to form the array with a 360-degree beam steering capability along the orbital plane. The satellite has no moving parts, weighs 2,000 t, and would deliver 2 GW of DC power to the grid from GEO via a 2.45 GHz microwave beam. CASSIOPeiA has also been investigated by the UK government as a way to de-risk their transition towards green electricity generation and looks likely to be pursued further after positive results from recent studies (Way & Lamyman, 2021b).

#### *MR-SPS:*

The Multi-Rotary joints Solar Power Satellite (MR-SPS) was first proposed in 2014 by China and recently updated in 2021 (Hou & Li, 2021). Out of our selected concepts, it is the only one that employs separated generation and transmission surfaces without any solar concentration. Therefore, it is comprised of freely rotating solar arrays to adjust to the sun's position. These are then connected via trusses with 100 rotary joints and cabling to a transmission antenna, which emits microwaves at 5.8 GHz from GEO. It is by far the heaviest concept at 10,000 t of in-space mass and generates 1 GW of DC power that can be fed into the grid.

Other notable concepts include older architectures by NASA and a number of designs by Japan. However, Japanese agencies have mostly transitioned to researching key technologies such as WPT and not published any updated concepts with parameters recently. The California Institute of Technology is moving in the opposite direction. Having initially succeeded in advancing high-performance ultralight sandwich modules for planar arrays, they are now starting to develop their own full-system concept *Madonna* (2021).

### 1.3. A general SBSP system model

To analyse different SBSP architectures from a technological and ultimately also an economic perspective, a common system model is required along which we can structure our approach. These defined subsystems also need to reflect the biggest levers for technological and ultimately cost improvements. Therefore, LCOE calculations from the literature based on subsegments (e.g. Marshall, Madonna, & Pellegrino, 2021) informed our decision on where to draw system boundaries.

Consequently, we will divide SBSP into a space segment, WPT and necessary ground structures, and manufacturing as well as infrastructure. These segments are also indicated in

figure 1. The space segment contains all structures that are permanently placed in orbit, such as PV arrays, reflectors, propulsion systems, and antennas. The WPT subsystem also concerns the antenna, the transmission process, and the reception as well as reconversion of the beam. Lastly, we look at anything related to the construction, assembly, maintenance, and launch of the satellite.

Gauging their respective importance for and impact on LCOE, launch costs are repeatedly identified in the literature as one of the largest drivers in variance for system cost (e.g. Way & Lamyman, 2021b). Consequently, developments in the launch market will therefore receive particular focus in section 4. Additionally, total launch costs are also influenced by the maintenance requirements and satellite mass. Hence, we will focus some of our metrics for the space segment on mass- and lifespan-related performance. Furthermore, the mass of the space segment can also act as a proxy for manufacturing costs and therefore has a dual impact on overall costs. With these circumstances in mind, we can begin our analysis with the space segment.

## 2. Space segment

First, we focus on the satellite or space segment of SBSP systems. While the antenna transmission array is part of our definition of the satellite, it overlaps with the wireless power transfer subsystem and is discussed in more detail in section 3. Hence, the consideration of components pertaining to the transfer of wireless power, such as the transfer antenna apertures, will only extend to their interaction with the overall satellite structure and design. This includes to some extent DC-to-RF conversion efficiencies to calculate metrics based on the satellite's RF power output as well as the implications of building an array of sandwich panels, which are discussed in section 2.5. DC-to-RF efficiencies are then addressed more directly in the subsequent chapter. Due to the lack of laser based SBSP transmission systems in the literature, a dynamic further investigated during the chapter on power beaming, our analysis for the space segment will exclusively focus on microwaves as a transmission modality. Overall, particular focus is placed on the PV cells and concentrators, module design, satellite structure, and the overall array management. We will also briefly discuss the impact of different choices of orbit.

### 2.1. Metrics for space segment evaluation

When comparing metrics for the space segment, it is important to be clear on which measurements are being used. For example, some PV prototypes on which metrics are reported do not yet include the transmit antenna array, hence reducing overall mass. It is also necessary to distinguish between installed solar power, RF power, and power delivered to the grid. Keeping this in mind, the following five metrics have been identified from the literature (e.g. Jaffe, 2020) as key determinants of space segment performance:

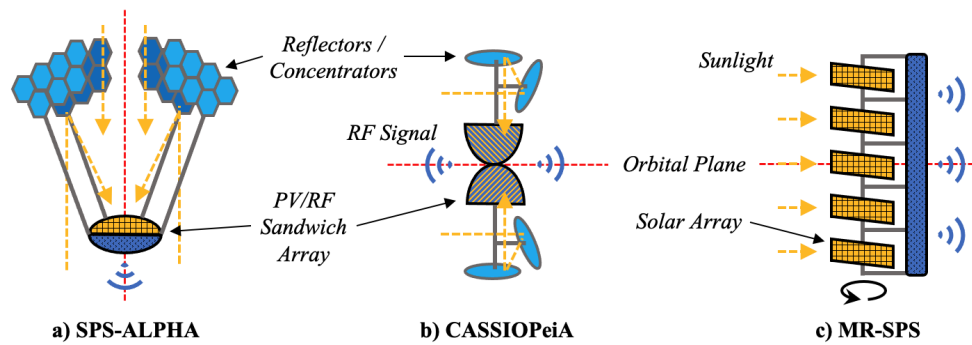


**Figure 2:** The satellite architectures of the three chosen concepts display significant differences in their approach on solar collection, conversion, and RF transmission. Own representation based on a) Mankins (2017), b) Cash (2019), and c) Hou and Li (2021).

*Collect/transmit area-specific mass [g/m<sup>2</sup>]:*

This metric, also known as areal density, puts the surface areas of collection plus transmit apertures in relation with the overall weight of the space vehicle. Only collect and transmit areas are considered, as otherwise external reflector and concentrator structures with large surface areas but little weight could greatly distort this number. Generally, a decrease in area-specific weight is connected to a decrease in launch costs, manufacturing costs, and to a lesser extent an increase in transmit efficiency (Marshall et al., 2021). The mass is mostly driven by structural components such as any necessary trusses and booms, the solar and antenna modules, and the electronics. If the surface area is complex to determine, it is sometimes reported in square meters intercepted sunlight.

*Mass-specific power [W/g]:*

Mass-specific power measures the amount of mass that needs to be placed in orbit to achieve a given power level. Just as with the area-specific mass, weight is a key determinant of the economics of SBSP and here it is set in relation to the benefits gained in the form of power. For this metric, it is particularly important to distinguish between installed solar capacity and transmission capacity after additional conversion losses. We will refer to them as PV power and RF power, respectively. It is also essential to match PV power with PV weight and RF power with PV plus RF system weight to compare like with like and include all components necessary to achieve a certain power level. The power fed into the grid on the ground is unsuited for calculating specific power metrics used to compare space segments, as it is influenced by the parameters of the rectenna on earth. To allow for comparability, we will reference PV or RF power capacity of the space vehicle, depending on whether the focus is on the entire structure or just the solar part. Furthermore, many innovative prototypes for SBSP PV technologies have not fully integrated power beaming devices during their demonstrations. As a result, such experiments will provide an upper bound for mass-specific power levels given a certain technology and are hence still of relevance to our discussion. There

might also be a trade-off between mass- and area-specific power, depending on whether launch capabilities are more constrained by weight or volume. However, the technologies discussed below suggest that weight might presently be a more determining factor, and hence we have chosen to put a larger focus on mass-specific power for the space segment. Together with the duty cycle, mass-specific energy can then be calculated.

*Duty cycle [%]:*

The duty cycle is measured as the share of one orbital rotation during which the SBSP can actively generate and transmit energy. Not only does this ratio depend on the structure and design of the satellite but also on the orbit to which the space segment is deployed. GEO is the orbit most commonly associated with SBSP concepts as it offers a theoretical duty cycle of 100%, depending on the satellite structure.

*Conversion efficiency [%]:*

Conversion efficiency for the space segment can either be measured from solar radiation to DC or DC-to-RF. For the solar components, cell efficiency also does not equal panel efficiency due to the wiring and other peripheral components. Efficiency is not only relevant to maximise the amount of power delivered to earth, but also in regards to heat management and consequently lifetime of the system. Generally speaking, the higher the efficiency, the less waste heat that needs dissipating will be produced.

*Operating lifetime [a]:*

The operating lifetime of the space asset is the amount of time the satellite can operate above a certain performance threshold. Of particular interest is the operating lifetime of key components, such as the solar cells. Here it is also seen as a proxy for the ability of the subsystems to deal with the harsh thermal and varying radiative environments present at all feasible orbits. Space maintenance capabilities also play a significant role in preserving the lifetime of the overall system. Nonetheless, the longer a component can function without the need for a replacement part, the fewer elements need

to be launched into space. Hence, the operating lifetime of components impacts the total mass that needs to be sent into orbit over the lifetime of the system.

To ensure that comparisons of metrics drawn from the literature are appropriate, some had to be recalculated or adjusted based on the disclosed data. For instance, a paper might report a mass-specific power metric for which only PV power but total sandwich module mass (including the antenna) was used. This number would not be suited for comparisons with metrics using only PV power and PV system mass or RF power and PV system plus antenna mass. Consequently, we had to recalculate some metrics based on the numbers reported with the demonstration results or adjust them based on data from other academic publications. To ensure metrics are adjusted following shared rules, we establish a common antenna weight premium that is added to purely PV-related technology options. This premium then allows us to determine an estimated mass for when these solar components are integrated into a sandwich module. The same concept applies for a structure premium, which accounts for supporting structures as well as deployment mechanisms and is added when individual sandwich modules are combined into a lightweight planar array. When applying these premia, it is assumed that the functional surface area stays constant. We also introduce common formulas to calculate mass-specific power and aerial density variants. These common formulas form the basis for any potential adjustments to ensure metrics include and exclude the same parameters when compared. The applicable formulas are introduced at the beginning of each subsection. A summary of all calculations is presented in section 2.7.

## 2.2. Photovoltaics

Solar power has a long history of being the energy source for projects in space, starting with the first solar-powered satellites Vanguard 1 and Sputnik 3 in 1958 (Andreev, 2018). Activity in space poses a number of demanding requirements to photovoltaic systems. They need to be lightweight, efficient and reliably operate for long periods of time in harsh conditions (Espinete-Gonzalez et al., 2019). The space environment is characterized by high and low energy particle radiation, large thermal cycles, high UV light exposure, and the possibility of collisions with space debris of any sort.

Having initially started with single-junction cells with only one junction to induce a flow of electrons, the most efficient cells today also used in space have multiple layers. These III-V multijunction cells are made from metal organic compounds of Group III and Group V elements, from which their name is derived. By correctly matching the subcell layers, thermal and transmission losses can be minimized (Philipps, Dimroth, & Bett, 2018) and as a result, power conversion efficiencies of the cells have increased to more than 50% over the last couple of years (Kalyuzhnyy et al., 2020). One of the techniques enabling the improved performance is photon recycling, where reflectors are placed to allow a second pass-through of unabsorbed photons through the photoactive region (Andreev, 2018). Specifically for

multijunction cells, Bragg reflectors made of multiple semiconductor layers increase the absorption length of sunlight. Additionally, they also increase the radiation resistance. Consequently, great efficiencies, high reliability, a relatively high mass-specific power, and excellent radiation hardness have led to III-V multijunction cells commonly being used for satellites and space vehicles (Philipps et al., 2018).

In space, such cells are often used in conjunction with concentrators. By focusing light that would normally have impinged on a wider area on a smaller part of the cell, they are critical in keeping efficiencies high, reducing the amount of required cell material, and provide indirect radiation protection to the peripheral components (Andreev, 2018). Crucially for SBSP, they can also increase mass-specific power if lightweight materials are utilized and are necessary to achieve specific powers above 1 W/g (Warmann et al., 2020).

However, despite these benefits, problems remain. So far, space solar power was mostly designed around keeping an aperture running as efficiently and reliably as possible. With SBSP, this goal shifts towards the cost-efficient production of renewable energy for earth. Hence, factors determining the economics rise in importance. Weight is one of them, especially given that solar panels are typically the heaviest component of a satellite (Abdelal, Gad, & Abulfoutouh, 2013). The weight of the cells themselves has already been cut with the introduction of thin-film variants, using thinned substrate (Law et al., 2006) and epitaxial lift-off technologies (Kayes, Zhang, Twist, Ding, & Higashi, 2014). Nonetheless, mass-specific power seems limited below 0.5 W/g (Gibb, 2018). Radiation shielding in the form of a cover glass placed on top of the cell is responsible for a significant part of the remaining weight (Espinete-Gonzalez et al., 2019). Hence, the cover glass necessary for today's most efficient GaAs multijunction cells is constraining mass-specific power and increasing area-specific mass. Nonetheless, ensuring an adequate useful lifespan by preventing degradation by radiation is also vital. This is especially the case for SBSP concepts in MEO, where the radiation environment is harsher than in GEO (Larson & Wertz, 1992). Different orbits and their implications are further discussed in section 2.6.

A second problem with current high-performance space cells is the reliance on geometric concentrators. As a result and as discussed in section 1.2, many modern SBSP designs include additional heavy concentrator structures comprised of booms and trusses to focus sunlight onto the solar cells without any intermittency or larger attitude adjustment maneuvers. Standard geometric concentrators also need to be pointed correctly to be effective, potentially requiring movable mechanisms constituting a potential point of failure. Other concepts also include additional on-chip concentrators (Cash, 2021a).

To measure the impact of these variations, we must first define common formulas for the mass-specific PV power  $p_{PV}$  and aerial density  $m_{PV}$ . Therefore, we designate these for-

mulas for the PV part of the satellite as follows:

$$p_{PV} = \frac{P_{PV}}{M_{solar}} \quad (1)$$

$$m_{PV} = \frac{M_{solar}}{A_{PV}} \quad (2)$$

$$M_{solar} = M_{SPG} + M_{reflectors} + M_{concentrators} \quad (3)$$

$M_{SPG}$  denotes the mass of the solar power generating components and together with any reflector structures or concentrators thus forms the simplified total mass required to achieve the nominal solar power output of a system. Some brief calculations can now show the impact reflectors and concentrators can have on area-specific mass and mass-specific power in particular as well as provide us with some points of reference for our further analysis.

The SPS-ALPHA concept has a total orbital mass of 7,600 t with 3.4 GW of solar power installed across a surface area of about 2.2 km<sup>2</sup> (Mankins, 2021). The solar power generating units only make up about 5% of total mass (Mankins, Kaya, & Vasile, 2012) and hence theoretically achieve more than 8 W/g at 181 g/m<sup>2</sup>. However, once the weight of concentrator and reflector structures is added in accordance with equation 3, this number nearly falls by a factor of ten to 0.95 W/g at about 1,600 g/m<sup>2</sup>. This illustrates the desirability of concentrator PVs without bulky external structures, a concept we will investigate in sections 2.2.1 and 2.2.2.

Another example is the Chinese MR-SPS system. Due to its reliance on separate PV and antenna surfaces, it also requires great amounts of framing architecture. The total orbital mass exclusively attributable to the 2.4 GW of solar power generation is 2,000 t (Hou & Li, 2021). Despite a significantly lower density of 333 g/m<sup>2</sup>, the resulting 1.20 W/g lie relatively close to the SPS-ALPHA concept due to the comparatively low power levels of MR-SPS. One reason for this might be the necessity of routing all the generated electricity through cables and slip rings to the antenna, which constraints the amount of power that can be installed to limit maximum voltage. Consequently, there is also no solar concentration employed. Mass-specific PV power would fall by half if the framing architecture were to be added to the equation.

Lastly, we will briefly look at the CASSIOPeiA concept, which reports a relatively light total orbital mass of 2,000 t and the collection of 11.3 GW of sunlight (Cash, 2021a). Accounting for optical losses of 20.1% due to multiple concentration steps and a PV cell efficiency of 39.4%, this results in 3.6 GW of PV capacity. Unfortunately, no further breakdown of satellite weight was available at the time of writing. Therefore, we can use the weight split of SPS-ALPHA as an approximation, with reflector and concentrators structures contributing 42% of total weight (Mankins, 2021). Based on the space segment architecture of CASSIOPeiA, where PV and antenna elements are jointly placed on the helical array,

we assume a 50/50 split for the remainder. Consequently, specific PV power in accordance with equation 1 equals 2.51 W/g at 491 g/m<sup>2</sup>. This can be considered very competitive compared to the other two concepts. However, the weight of external structures again decreases the metric by a factor of two to three, strengthening the case for a different approach to concentrator PVs for SBSP.

It should also be noted that neither of the three systems has an operational prototype and instead all fully rely on modelling to obtain their metrics. Hence, the numbers are theoretical and could decrease further in practice. In section 2.3 on module design, we also investigate similar dynamics when calculating performance indicators that include antennas and additional components. An overview of all metrics will then be provided in section 2.7. With the results above as a first point of reference for collect area-specific mass and mass-specific PV power, we can now investigate some technology alternatives that show promise in overcoming some of the aforementioned problems.

### 2.2.1. Integrated geometric concentrators

One possible solution to eliminate heavy supporting structures is to integrate concentrators directly onto the PV module. Such attachments could theoretically work in addition to any on-chip concentrators. One of the most successful designs replaces standard planar cell area with parabolic silver mirrors fabricated from ultralight carbon fibre reinforced polymer (CFRP) optics (Warmann et al., 2020). Each mirror would concentrate light onto the back of its neighbour, where a strip of PV cells including a cover glass is situated as pictured in figure 3. Additionally, a multilayer optical coating is applied to each mirror to aid with heat dissipation for cell cooling. As a result, cell temperatures can be kept below 100 °C despite the concentration. Heat management is particularly important for promising new cell materials as discussed in section 2.2.3.

It should further be noted that there is an inverse relationship between the level of concentration and the maximum acceptance angle under which sunlight can be gathered. While higher concentration increases specific power, it also constraints the angle from which sunlight can still be accepted. This trade-off has implications for overall module and system design as well as the power-optimal guidance of the structure.

Overall, on-module curved silver mirrors have greatly boosted specific power during experiments conducted by Warmann et al. (2020). The prototype module also included the RF components necessary for transmission but omitted any supporting structures required to form an array. We will return to the set-up including transmit antennas in section 2.3.1.

As part of the experiment, points of reference were established. Commercially available cover glass-interconnected cells (CICs) without any concentration displayed a mass-specific PV power of 0.54 W/g at 804 g/m<sup>2</sup> (Warmann et al., 2020). As a base for the concentrators, a mass-optimised multijunction space cell comprising a cover glass was used,

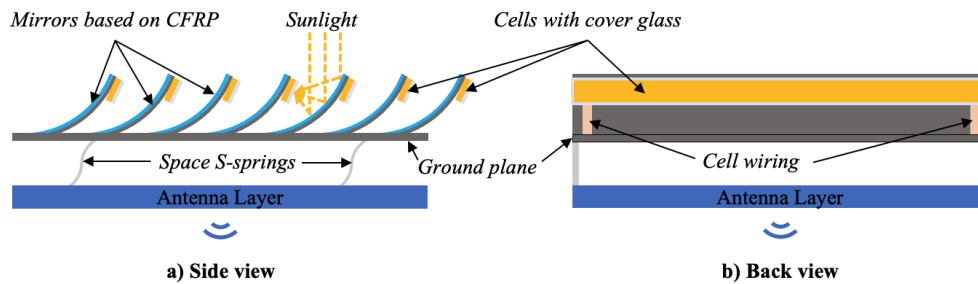


**Figure 3:** Visualisation of the ultralight concentrator concept by Caltech with parabolically curved mirrors concentrating the light onto strips of PV cells on the back of the neighbouring mirror. An integrated DC-to-RF and antenna layer has also been added. Own representation based on Warmann et al. (2020).

which on its own achieved 1.00 W/g at one sun and nearly half the area specific weight of 450 g/m<sup>2</sup>. The addition of such a cell to a 7.5 sun concentrator structure, such as shown in figure 3, nearly quadrupled the result to 3.75 W/g at 116 g/m<sup>2</sup>. Doubling the concentration factor to 15 suns and making the mirrors thinner led to another increase to 5.20 W/g at 83 g/m<sup>2</sup>. By altering the coating on the concentrators, allowing the mirrors to be even thinner and hence lighter, a final increase of specific power to 5.90 W/g at only 67 g/m<sup>2</sup> was observed. This constitutes a significant improvement compared to the commercially available cells by around a factor of ten. Efficiencies were very similar at about 30% across all tested system compositions. The results also show significant improvements compared to the initial prototype tested two years earlier, which achieved only 0.23 W/g at 800 g/m<sup>2</sup> (Kelzenberg et al., 2018). In comparison with some of the SBSP concepts, these measurements suggest that intelligently integrated concentrators could greatly boost the metrics critical for PV performance by increasing solar power levels while eliminating considerable amounts of mass.

Nonetheless, significant hurdles remain with the parabolic concentrator structures. Firstly, some of the ultrathin CFRP materials used in the demonstration are not yet commercially available, which renders mass-manufacturing capabilities uncertain (Warmann et al., 2020). Furthermore, volumetric structures on top of the module constrain overall system architecture due to PV capabilities being limited to only one side. Together with constraints on the acceptance angle under high-concentration scenarios, particularly accurate attitude management of the solar array would be required (Madonna, 2021). Lastly, they also complicate manufacturing processes overall and suffer from optical losses. Consequently, researchers have also been looking at other integrated concentrator alternatives which allow for planar PV structures. Depending on the SBSP system design, the benefits of maintaining a planar structure to enable dual-sided modules can be substantial and are further discussed in section 2.3.

### 2.2.2. Luminescent solar concentrators

To maintain a flat-plate architecture while keeping specific power high and area-specific weight low, a different approach is required. Developing photonic devices with characteristics at the nano-scale opens up possibilities for new non-geometric concentrators by taking advantage of elemental interactions between light and matter. Luminescent solar concentrators (LSCs) make use of luminophores in the form of quantum dots, which emit photons when excited by short-wave light or ionising radiation (Needell et al., 2017). Quantum dots are nano-scale material structures made from semiconductors whose extremely small scale leads to changes in their optical and electronic properties based on quantum mechanics. These can then be manipulated for the purpose of concentrating solar irradiation on a PV cell by embedding them into an optical waveguide. The resulting architecture is displayed in figure 4. When hit by radiation passing through the layers of the array, the luminophores then emit light which is directed towards a PV micro-cell by the waveguide. Through selectively picking the semiconductor materials of which the quantum dot is composed, it is possible to influence the bandwidth of wavelengths in which light is emitted. This bandwidth can then be optimized for the chosen solar cell to maximize efficiency, for example by down-converting blue or near-UV light to red (Madonna, 2021).

While photovoltaic systems utilizing standard geometric concentrators, such as described in section 2.2.1, are particularly bad at capturing diffuse sunlight, LSCs can absorb direct and diffuse sunlight (Needell et al., 2018). Therefore, quantum dots can not only eliminate the need for concentrator structures but also boost efficiency further by capturing more of the light available. These benefits have also been observable in device modelling simulations utilizing LSCs, after first tests in 2018 indicated that quantum dots could notably improve conversion efficiencies (Needell et al., 2018). Without bandwidth optimization of the light emitted by the luminophore, mass-specific power levels of above 1 W/g at 140 g/m<sup>2</sup> and conversion efficiencies of about 12% have been achieved (Needell et al., 2019). By using spectrally-optimized quantum dots, specific power values were nearly doubled to 1.84 W/g at the same area-specific mass and efficiencies improved to close to 20%. Other simulations sug-

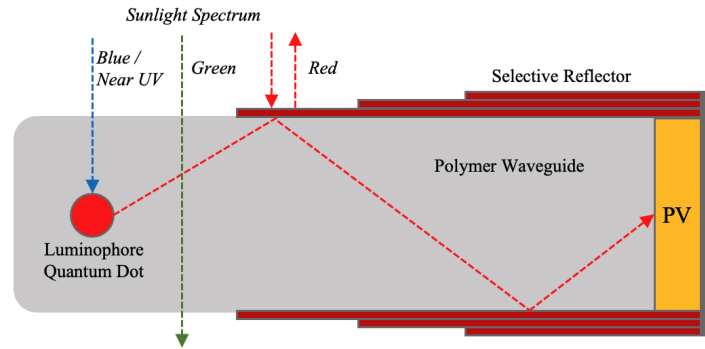


**Figure 4:** Luminescent solar concentrators employ a quantum dot made from a luminophore which emits light of specific wavelengths when excited by radiation. This light is then directed towards a solar cell by the waveguide. In this example, near UV light passing through a selective reflector is converted to red light by the quantum dot before being transmitted to the PV cell. Own representation based on [Madonna \(2021\)](#).

gest that, under optimal conditions, power conversion efficiencies of around 30% are well within reach ([Needell et al., 2017](#)). In first tests, LSC cells have also exhibited higher radiation tolerances due to a reduction in their effective cross section ([Hu et al., 2021](#)).

Therefore, quantum dot cells appear to be a promising option for delivering radiation resistant flat-plate concentrator PV modules. LSC technology can also be integrated into flexible PV sheets ([Needell et al., 2019](#)). This characteristic is greatly beneficial for space solar module designs that rely on folding or coiling to keep volumes small during launch. A material of particular interest for these types of flexible quantum dot cells has been perovskite. Despite their relatively early stage of development, flexible LSC perovskite cells have achieved efficiencies of more than 12% and displayed greater mechanical endurance than standard thin-film PV cells ([Hu et al., 2021](#)). A research grade device of this kind is set to fly for tests in 2022 ([Madonna, 2021](#)). Additional benefits of perovskite are discussed in more detail in the following section.

However, while LSC modules are certainly promising, it should be noted that simulations did not include any connecting or transmission structures, which naturally decreases weight. We will address this in the conclusion of this chapter by utilizing the calculated weight premia. Additionally, two limitations that were frequently encountered are the absorption of the light by the luminophore as well as poor trapping of the emitted light by the waveguide ([Needell et al., 2018](#)). Both of these result in less solar energy reaching the PV cell and have to be investigated going forward. Lastly, their exact behaviour under thermal and radiation stress has not been fully explored yet. Future research efforts will have to address these obstacles to make LSC cells ready for SBSP systems, given the promise they are showing in attaining high mass-specific power levels while maintaining a planar module geometry.

### 2.2.3. Perovskite cells

Researchers are continuously exploring new material compositions with beneficial properties for the use in solar cells. One of the materials that has gathered particular attention over the last couple of years is perovskite. Solar cells based on perovskite display the ability to withstand high-energy proton doses that exceed the levels basic silicon cells can endure by almost three orders of magnitude ([Lang et al., 2016](#)). But not only is their radiation resistance higher, their self-healing properties mean that photocurrent and photovoltaic performance of the cell also start to recover over time. This process based on thermal annealing even starts when performance has dropped to as low as 2% after high radiation exposure ([Madonna, 2021](#)).

The strong inherent radiation tolerance and high damage threshold would allow for the removal of the protective cover glass. Lightweight flexible perovskite solar cells manufactured this way have been tested under radiation conditions that equal several years of exposure in space, confirming their resilience and great potential for SBSP applications ([Malinkiewicz, Imaizumi, Sapkota, Ohshima, & Öz, 2020](#)). First prototype cells based on perovskite compounds have been able to achieve exceptionally high specific power values of 29 W/g at an efficiency of 15.2% ([Kang et al., 2019](#)). The aerial density  $m_{PV}$  was measured at a mere 4 g/m<sup>2</sup>, in part due to the lack of any heavy glass. While it should be noted that this was for a single prototype cell without any peripheral structures and electronics, the performance increase is still significant and would even remain very competitive with mass increases by a factor of ten or more. However, at about 20%, power conversion efficiencies still notably lag behind those of standard multijunction cells ([Kim et al., 2017](#)).

Nonetheless, perovskite cells also display problematic characteristics. Thermal degradation already starts to occur at 85 °C ([Kim et al., 2017](#)), with performance deteriorating in less than 24 hours to the point of inoperability as a result ([Miyazawa et al., 2018](#)). This is particularly problematic as the solar panels of satellites are known to be one of the

parts most exposed to severe thermal cycles, reaching temperatures of up to 125 °C (Pisacane, 2005). While progress has been made in composing cells that are more stable and can manage elevated temperatures for extended periods of time, the conversion efficiencies of these variants have so far remained very low at under 5% (Miyazawa et al., 2018).

In conclusion, perovskite solar cells are still relatively early in their development compared to modules based on other materials. Still, more research should and is being conducted on how to keep the coveted characteristics while overcoming some of the shortcomings, given the great promise these first forays have shown.

#### 2.2.4. Nanowires

Besides for the purpose of solar concentration, operating at the nano-scale can also be exploited to achieve greater radiation resistance. Having inherently radiation-resistant materials that require minimal additional protection in the form of heavy cover glass can potentially boost specific power ratios more than simple efficiency gains (Gibb, 2018). Based on this idea, material or structural compositions that trade efficiency for radiation resistance in order to eliminate the cover glass and extend the operating lifetime are of particular interest.

One technology that follows this approach are nanowire PV cells. Nanowires are one-dimensional nanostructures used for electrical transport (Cui, Duan, Hu, & Lieber, 2000). Therefore, they effectuate the same purpose as normal wires in standard cells but at a much smaller scale. Together they form an array of high-aspect-ratio semiconductor structures with particular dimensions to enhance light absorption and radiation resistance (Barrigón, Heurlin, Bi, Monemar, & Samuelson, 2019). Simulations have shown the great potential of this technology to provide efficient, lightweight, and radiation-tolerant power generation units in space (Espinet-Gonzalez et al., 2019). These findings could then be confirmed by experiments, in which nanowire cells displayed a damage threshold that was 10 to 40 times higher compared to standard planar control cells. Upon closer inspection, this benefit seems to result from a reduction in effective cross section susceptible to defect production, much like with LSCs. In other words, by using wires at the nano-scale arranged in a particular fashion and embedded in the right materials, these cells present a substantially smaller area where impingement by incoming high-energy particles would lead to degradation. They also benefit from the fact that they are otherwise made of the same materials as standard III-V multijunction space cells.

Tests under space conditions were further able to corroborate these findings, with efficiencies ranging from 15% to about 18% and improving over time (Espinet-Gonzalez et al., 2020). Researchers also expect potential for optimization with regards to the array geometry, which could further boost efficiencies and radiation tolerances. Nonetheless, these numbers are the evidence of a for now necessary trade-off between efficiency and radiation tolerance compared to standard planar arrays. Lastly, nanowire arrays can

also be produced in the lightweight flexible sheet form conducive to packaging and deployment in space (Cavalli, Dijkstra, Haverkort, & Bakkers, 2018). Overall, they provide the possibility of extending operating lifetimes while eliminating the cover glass for SBSP applications, in turn increasing specific power through a reduction in specific weight.

While the exact magnitude of these gains will have to be validated through additional prototype testing, some brief calculations can show the potential. We assume that nanowire technology will offer the possibility of completely eliminating the cover glass used for a specific cell. In reality, this will likely only be possible in tandem with some of the other technologies introduced in this section. However, for simplicity, we will fully attribute the potential benefits to nanowires for the purpose of establishing an upper bound. Expecting a convergence of efficiency levels over the long term and knowing that the cover glass can account for about two thirds of total PV mass (Xu, Li, Tan, Peters, & Yang, 2018), we use the commercially available CIC from Warrmann et al. (2020) to recalculate mass-specific PV power with the weight reduced by two thirds. The result of 1.56 W/g suggests that nanowire cells bear the theoretical potential of tripling  $p_{PV}$  from initially 0.54 W/g by decreasing aerial density of the CIC from 804 g/m<sup>2</sup> to 278 g/m<sup>2</sup>.

#### 2.3. Module design

While reliable and lightweight PV is critical for the functionality of the space segment, it is at least of equal relevance how the solar elements are integrated into modules with the other satellite components, notably the transmission devices. The importance of such modularity is further addressed in chapter 4.2. In this section, we introduce various design options and their effect on weight- and power-related metrics. Possible satellite structures and resulting deployment dynamics will be discussed in the subsequent section.

Including the RF infrastructure of the space segment into our analysis requires us to expand our equations from section 2.2. Adding the mass and surface area of transmission hardware components as well as considering the RF power output of the satellite yields the following formulas.

$$P_{RF} = \frac{P_{RF}}{M_{solar} + M_{RF}} \quad (4)$$

$$m_{RF} = \frac{M_{solar} + M_{RF}}{A_{PV/RF}} \quad (5)$$

$$P_{RF} = P_{PV} * \eta_{DCRF} * \eta_{antenna} \quad (6)$$

$$M_{RF} = M_{DCRF} + M_{antenna} \quad (7)$$

The index  $DCRF$  denotes the infrastructure necessary to convert the DC power generated by the solar array into RF power, which is then transmitted by the antenna. In some

publications  $\eta_{DCRF}$  also already includes  $\eta_{antenna}$ . Additionally,  $A_{PV/RF}$  varies depending on the satellite design. For sandwich modules, which have a shared collect and transmit structure, equation 8 applies.

$$A_{PV/RF} = A_{PV} = A_{RF} \quad (8)$$

For separate solar and transmission structures, such as with the MR-SPS concept,  $A_{PV/RF}$  is defined by equation 9.

$$A_{PV/RF} = A_{PV} + A_{RF} \quad (9)$$

The different metrics reported in Warmann et al. (2020) for modules with and without the RF component also allow us to determine a general weight premium for adding transmission infrastructure to a lightweight solar module. The magnitude of this change is therefore measured at 29 g/m<sup>2</sup>. This premium can then be used heuristically to turn standard PV modules into integrated sandwich modules and vice versa. We have therefore established a common baseline for calculating the metrics selected to compare different satellite module designs.

### 2.3.1. Sandwich modules

As discussed in section 1.1, most historical SBSP designs relied on separate solar collection and power transmission surfaces. Even today, the Chinese MR-SPS system still relies on an external antenna connected to the solar array via rotating joints (Hou & Li, 2021). However, there are two major problems arising from such an approach. First, the 6-km<sup>2</sup> large solar array requires extensive wiring to route the electricity to the point of transmission. Second, the for accurate targeting necessary independent rotation of both surfaces requires something like a slip ring mechanism, which will be under considerable thermal stress and constitutes a single point of failure (Jaffe, 2020). Therefore, almost all modern designs envision the use of so-called sandwich modules to drastically reduce overall weight, in line with the trends we have seen for solar components. These integrated modules, which allow for the elimination of a majority of the wiring and supporting structures during the DC-to-RF conversion process while also introducing more redundancy to the system, can be used in conjunction with lighter PV and transmission technology to achieve higher specific power levels. The California Institute of Technology is one of the leaders in the area of planar sandwich modules, thanks to its extensive research efforts as we will see below.

Generally speaking and as the name suggests, sandwich modules consist of multiple layers, each of which dedicated to one of the key functions of a SBSP satellite (S. A. Hajimiri, Atwater, Pellegrino, Abiri, & Bohn, 2021). Hence, there are at least three layers as shown on the left in figure 5. One for PV-to-DC, another for generation of the microwave signal or DC-to-RF, and a third for the transmission of the signal. Additional layers might be required, e.g. for beam control. Together, they form a module that acts as a solar-powered space-borne transmit antenna, sometimes

called a spacetenna (Jaffe, 2020). As a result, routing distances are minimized, heavy cables and many supporting structures eliminated, and the spacetenna is deconstructed into many identical individual parts (Madonna, 2018). Such modularity also has significant implications for manufacturing and maintenance as discussed in section 4.2. For some applications it can be advantageous to rearrange the layers of the sandwich module from a flat tile into an L-shape (Jaffe, 2013) as shown on the right in figure 5. However, this only changes the geometry due to added optics but not the underlying functionality of the panel as the elements still share a common substrate and are therefore nonetheless considered a sandwich module.

The idea of sandwich architecture was first introduced by Owen Maynard as part of early SBSP studies by NASA and the Department of Energy (Maynard & Blick, 1980). Since then, first prototypes were introduced by Japanese researchers around the turn of the millennium (Matsumoto, 2002) and later further developed at Kobe University (Etani, Iwashita, & Kaya, 2011). Unfortunately, metrics relevant for specific power or aerial density calculation were reported for neither of the two. Another prototype was built at the U.S. Naval Research Lab (NRL) and tested in realistic space conditions with varying illumination (Jaffe, 2013). However, mass-specific power remained rather subdued due to a very high aerial density of 21.9 kg/m<sup>2</sup>, resulting in merely around 0.005 W/g.

Significant progress has been made since, as evident by the sandwich modules developed by Warmann et al. (2020) and introduced in section 2.2.1. Once the conversion infrastructure and an antenna were added to the PV section, as displayed in figure 3, even a mass-optimised multijunction cell without any concentration still achieved a mass-specific RF power  $p_{RF}$  of 0.67 W/g at 476 g/m<sup>2</sup>. With concentrators and the lightweight redesign, the metric went up to 2.87 W/g at 96 g/m<sup>2</sup> for these kind of sandwich modules. While the specific RF power level is less than half that of  $p_{PV}$ , it can still be considered as quite competitive. However, it should also be noted that many prototypes have only integrated the elements indispensable to the solar-to-RF process and are missing phase shifting equipment or sometimes even a functioning antenna. Therefore, slight weight increases should be expected for a SBSP-ready sandwich module.

In comparison, the Chinese system with its separated generation and transmission surfaces, only achieves 0.27 W/g in mass-specific RF power when including PV and antenna systems but excluding supporting structures (Hou & Li, 2021). These calculations suggest that combining both surface areas via sandwich modules could significantly increase the relevant performance indicators of the space segment.

Nonetheless, the way in which the module layers are integrated and the weight of the antenna components also matters. The SPS-ALPHA concept envisions hexagonal frames to combine the functional layers (Mankins et al., 2012). These frames add a lot of mass to an otherwise relatively light sandwich design. Consequently, mass-specific RF power falls to 0.33 W/g at a comparatively heavy 3,222 g/m<sup>2</sup>.

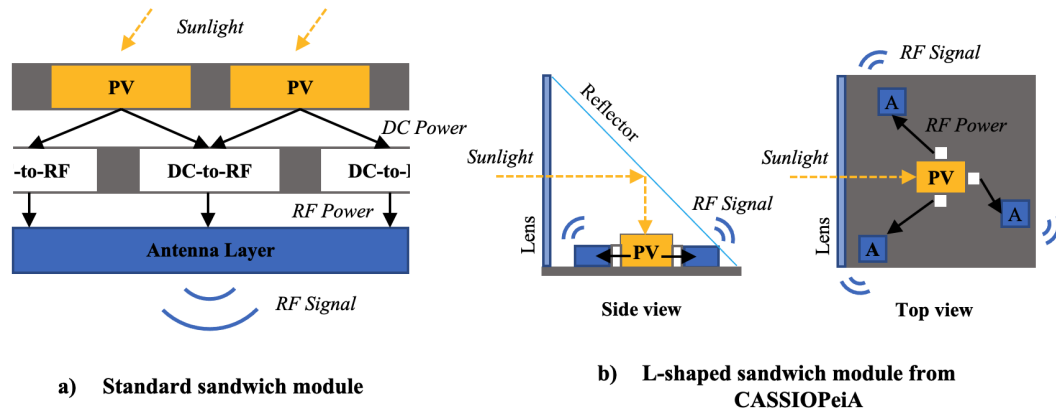


**Figure 5:** The integrated layers and components of two variants of sandwich modules. The strategically placed antennas in b) allow for 360-degree beam steering on the horizontal plane. Own representation based on a) [Madonna \(2018\)](#) and b) [Cash \(2017\)](#).

For CASSIOPeiA, we still have to include the helical array structure to which the modules are affixed due to a lack of granular data. Nonetheless, it achieves a notable  $p_{RF}$  of 1.51 W/g at only 692 g/m<sup>2</sup>, even including these structures. The fact that CASSIOPeiA therefore outperforms the MR-SPS by a factor of three further suggests that the benefits of well-integrated transmission and collection surfaces are substantial.

An improved version of the sandwich prototype proposed by [Jaffe \(2013\)](#) has also recently been sent for in-space testing with the help of the X-37B orbital test vehicle ([NRL, 2020](#)). During the NRL's Photovoltaic Radiofrequency Antenna Module Flight Experiment (PRAM-FX), the test vehicle ascended to LEO to observe conversion efficiencies under space conditions. The modules were also occasionally heated to demonstrate the thermal conditions in GEO. Preliminary results suggest DC-to-RF efficiencies of 37.1% and PV efficiencies of 22.6%, resulting in a rather low overall module efficiency of 8.4% ([Rodenbeck et al., 2021](#)). This is symbolic for some of the issues that remain with such tiles.

Space segment design relying on sandwich modules also has inherent shortcomings. Integrating all functionalities and consequently the materials into a single tile can prove difficult while maintaining high efficiencies and pose problems for heat dissipation ([Jaffe, 2020](#)). Hence, the efficiency of each layer becomes even more important to minimise thermal losses. Another issue is the correct alignment of the individual tiles. The structure resulting from these individual modules is susceptible to applied forces such as microgravity and therefore requires in-situ surface shape measurement to maintain beam control ([Madonna, 2018](#)). This issue of array management is discussed in section 2.5.

Furthermore, the orientation of the sandwich structure during its orbit to ensure continuous operation can pose problems. Seeing how solar and antenna surfaces can no longer be rotated independently of each other, simultaneous alignment towards the sun and the ground station becomes impossible for some orbital positions. For instance, the satel-

lite would not be able to transmit around local midnight, as the antenna surface would point away from earth if the solar side remains sun-referenced. This problem can either be addressed at the module design or the satellite structure level. For structural solutions, rear reflectors or mirrors combined with concentrators, such as the ones used in the SPS-Alpha ([Mankins, 2021](#)) or CASSIOPeiA ([Way & Lamyan, 2021b](#)) concepts, would trade additional weight for a continuous duty cycle. However, focussing light on the sandwich tiles also bears the risk of increasing any thermal challenges. In a more innovative approach, the CASSIOPeiA's helical arrangement could pose another potential solution. This structural concept is briefly examined in section 2.4.2. Another alternative on the design side are dual-sided sandwich modules, which we investigate next.

### 2.3.2. Dual-sided modules

One idea that has been investigated to overcome duty cycle limitations of planar structures comprised of sandwich modules are dual-sided tiles ([Marshall, Goel, & Pellegrino, 2020](#)). In general, this would result in the integration of either a second RF surface, a second PV surface, or both, allowing for increases of the duty cycle of up to 50%. These different configurations are displayed in figure 6.

In order for the supplementary layers to not block solar or RF functionalities on any side, they either have to be optically transparent RF or RF-transparent PV. Due to the transparency, adding both only results in greater module weight without any meaningful expansion of the duty cycle. With one dual-sided capability, it is already possible to optimise for the attitude of the single-sided element without compromising the functionality of the other layers. However, optically transparent antennas and particularly RF-transparent PV is technologically very challenging ([Madonna, 2018](#)). Hence, development so far has mostly focused on sandwich modules with an additional optically transparent RF layer, which also promises to be lighter than the alternative of transparent PV. Dual-sided RF furthermore benefits from shared DC-to-RF

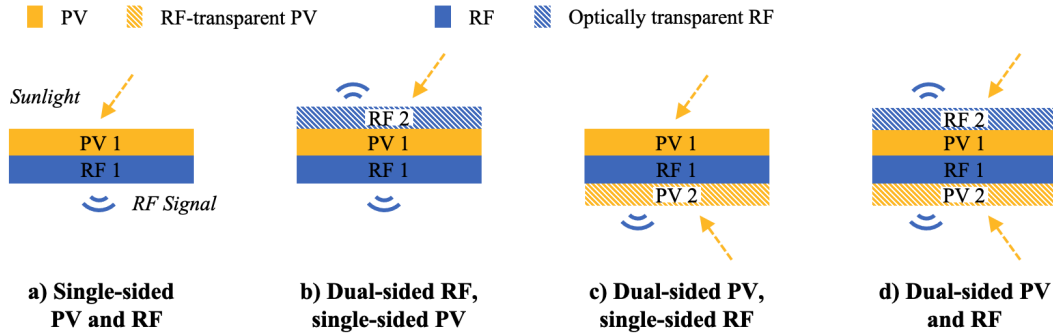


**Figure 6:** Sequential addition of transparent layers showcasing different possible configurations for dual-sided sandwich modules. The addition of one transparent layer as in b) or c) is enough to extend the duty cycle by up to 50% for planar arrays without rear reflectors. Own representation based on Marshall et al. (2020).

infrastructure.

Transparent antennas are not a completely new concept. Already in 2009, American researchers have experimented with mesh antennas placed on the solar cells of small satellites, achieving transparency levels of 93% (Turpin & Bakur, 2009). Overall, a meta study in 2020 was able to confirm that their performance had reached close to parity with non-transparent kinds (Silva, Valenta, & Durgin, 2020). Similar concepts have also been investigated by Chinese scientists (Qiu et al., 2021). Therefore, these findings suggest that adding an optically transparent RF layer appears to be a promising way to maximise the duty cycle of planar sandwich arrays without greatly increasing module weight.

However, even with dual-sided tiles in place, precise attitude control is still essential. This optimisation problem is also called power-optimal guidance and is based on a trade-off between a position that maximises power collection and a position that maximises power transmission while accounting for the permissible squint angles of both surfaces (Marshall et al., 2020). All these parameters also vary with the chosen orbit, with GEO displaying the greatest benefits from introducing dual-sided variants.

While no data on dual-sided RF module prototypes has been reported at the time of writing, we can once again use the CIC and flat-plate cell from Warmann et al. (2020) to calculate some approximations. Essential for this heuristic is the determination of a multiplier for the standard one-sided RF layer weight premium established at the beginning of this section. The fact that state-of-the-art optically transparent antennas are of a mesh-like structure and can share significant parts of the DC-to-RF conversion infrastructure of the other antenna suggests that the multiplier should be well below two. For the purpose of our approximation, we have chosen 1.3 as a suitable factor. Once these assumptions are applied to the cells' parameters, we obtain 0.28 W/g for the CIC and 0.51 W/g for the flat-plate variant. Both constitute a decrease of about 20% when compared to their standard sandwich configuration. This gives us a rough order of magnitude for the benefits an extended duty cycle would have to realize to outweigh the increase in weight. To fully capture

this dynamic, mass-specific energy might be a better metric for comparing single- and dual-sided sandwich modules. Nonetheless, additional research beyond models is needed to investigate whether overall the mass, cost, and complexity added by introducing additional layers ultimately overshadow any system efficiency gains (Marshall et al., 2020).

#### 2.4. Satellite structure and deployment

In this section, we explore different satellite structures into which the individual modules can be arranged. Some of our considerations from the previous sections, especially those on concentrators, will be of great relevance to the overall structure. In particular, we will explore the impact of the addition of trusses, booms, and any other structural elements necessary to form the space segment on its weight- and power-related metrics.

Our primary focus when it comes to SBSP satellite structures rests with planar and helical shapes, the latter addressing some of the shortcomings of flat-plate architectures. Lastly, we also consider any stowage and deployment mechanisms required to place the body in orbit, as these also impact satellite design and the selected performance metrics. Therefore, compact packaging and smooth deployment while adding as little weight as possible are essential.

Consequently, we will also have to add new variables for supporting structures to our equations to calculate overall satellite array performance. Mass-specific power and aerial density for the entire space segment will therefore be calculated in accordance with equations 10 and 11.

$$p_{satellite} = \frac{P_{RF}}{M_{solar} + M_{RF} + M_{structures} + M_{auxiliary}} \quad (10)$$

$$m_{satellite} = \frac{M_{solar} + M_{RF} + M_{structures} + M_{auxiliary}}{A_{PV/RF}} \quad (11)$$

For  $A_{PV/RF}$ , equations 8 and 9 still apply. The mass of auxiliary systems such as propulsion is represented by  $M_{auxiliary}$ . However, in most concepts they account for less than 1% of total mass, limiting their impact on  $p_{satellite}$  and  $m_{satellite}$ .

These formulas now allow us to determine the effect of including structures to form a stowable and deployable array out of individual modules.

#### 2.4.1. Planar arrays

Planar arrays combine a large number of sandwich tiles or modules into one common plane, which acts as a solar power collector and converter as well as transmission antenna in space. One envisioned approach for this is displayed in figure 7. A tile is seen as the basic unit of functionality of which many will be arranged and connected into a strip with 1 m in width and 60 m in length (Pellegrino et al., 2020). Attached to deployable booms, these then form a PV and RF space segment measuring 60 m × 60 m. Multiple of these space segments combined could make up a SBSP power station. Therefore, planar arrays are easily scalable by adding to the number of space segments. Consequently, sequentially increasing the size of any smaller prototype in space until commercial scale is achieved should be possible without greater issues.

Once again, the use of dual-sided tiles as discussed in section 2.3.2 would be essential to maximising the duty cycle of a planar space segment. So far, increases of up to 50% are expected compared to single-sided modules (Marshall et al., 2020). However, some intermittency would remain, requiring utility-scale storage on the ground to achieve constant power supply. Therefore, the overall trade-off for a planar satellite would be between significant advantages in terms of modular structure, scaling, and weight versus some remaining intermittency. However, large-scale storage is also critical for other more prominent renewable technologies such as wind and terrestrial solar. Hence, this is not an issue specific to SBSP and contrary to the other technologies, the intermittency associated with space solar would be very consistent and predictable over the entire lifetime of the satellite.

For large planar structures to be viable, a mechanism needs to be in place to allow for compact packaging during space launch and transport as well as the subsequent deployment. One approach would see the space segment being z-folded and rolled prior to launch, inspired by specific origami techniques called *kirigami* (Gdoutos, Leclerc, Royer, Türk, & Pellegrino, 2019). Following such a procedure, the nominally 60 m × 60 m payload could be transformed into a cylindrical package of 2.2 m diameter and 1.8 m height (Madonna, 2021). This is based on extrapolations from smaller scale lab studies using a 1.7 m × 1.7 m prototype (Gdoutos et al., 2020).

Once the orbit is reached, deployment is initiated by first uncoiling the cylinder and then unfolding the different strips (Pedivellano, Gdoutos, & Pellegrino, 2020). This is achieved by releasing strategically placed external constraints and subsequently letting the array self-deploy, using the elastic energy stored during packaging. Such an approach is also called strain-energy-deployed. Nonetheless, a 60 m × 60 m structure would have many folds susceptible to wrong or incomplete deployment. Therefore, the sequence in which the constraints are released needs to be optimised and controlled

to minimise chances of failure. First trials suggest that a step-wise deployment from the inner-most to the outer most strips of the space segment could be a viable option (Pedivellano et al., 2020).

Tests of space segments for such a satellite structure have already been able to provide some insights into the metrics, with an initial design in 2016 setting a target of 100 g/m<sup>2</sup>. A prototype with the dimensions of 1.7 m × 1.7 m managed to achieve 150 g/m<sup>2</sup> in 2018. At a share of 42%, the two longerons connected to each strip contributed the most to the system's overall mass (Gdoutos et al., 2020). The 50- $\mu$ m thick functional material followed closely behind at 41%. Functional area also makes up about 75% of the total area of the space segment. The result was an areal density of 136 g/m<sup>2</sup>, which is comparable to the levels discussed in section 2.3 on module design. Additionally, as the structure is scaled up to its commercial proportions of 60 m × 60 m, the weight share of supporting structures nearly halves to 24%, bringing area-specific mass down to 126 g/m<sup>2</sup>. Such numbers would be quite comparable to some of the other concepts such as SPS-ALPHA, where supporting structures at scale are responsible for a similar share of total mass (Mankins et al., 2012). However, SPS-ALPHA is still much heavier at an absolute level per module, suggesting room for improvement.

For the extrapolation of the commercial array, an aerial density of 100 g/m<sup>2</sup> for the functional material was assumed, in line with what has been achieved in past demonstrations of sandwich modules (e.g. Warmann et al., 2020). Based on the numbers reported by Gdoutos et al. (2020), we can assume that additional structures to form the space segment as well as for deployment and packaging would increase the aerial density of high-performance ultralight sandwich modules on average by 32 g/m<sup>2</sup>. This structural weight premium can now be used to heuristically calculate performance metrics for an array containing any type of sandwich module. For instance, adding structures to the flat-plate multijunction tiles from section 2.2.1 would lower mass-specific RF power only slightly from 0.67 W/g to 0.62 W/g. The impact is greater with lighter modules such as the 15-suns concentration variant, where specific power would decrease by about a fourth to 2.15 W/g. Such a value for  $p_{satellite}$  would still be significantly higher than CASSIOPEIA's mass-specific RF power for the entire satellite of 1.51 W/g. This suggests that the benefits of eliminating external reflector and concentration structures might be substantial. Due to their heavy components and architecture, SPS-ALPHA and MR-SPS only achieve 0.32 W/g and 0.16 W/g, respectively.

There are also efforts to eliminate even more connectors and hence mass by having the elements of the space segment fly in formation. For instance, the private company Solaren has patented one specific approach (Rogers & Spirmak, 2005). The idea is that power plants comprised of multiple space segments orbiting in formation would be even easier to scale and require less assembly. However, the power-optimal guidance problem becomes greater as the number of independent elements increases. First studies indicate that the elements of the constellation would also have to perform peri-

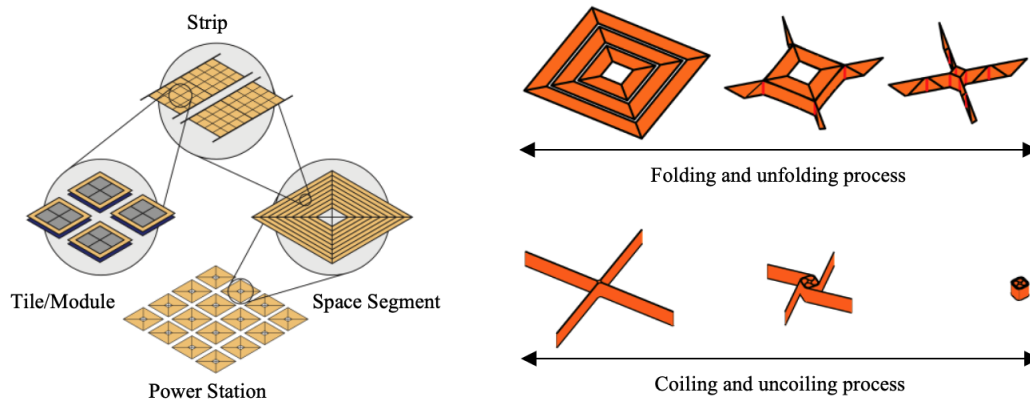


**Figure 7:** The left side is a visualisation of how individual tiles or modules form space segments which can be combined into a space power station. The right side shows the deployment mechanism for the space segments as a sequential combination of folding and coiling. Adaptation based on Gdoutos, Truong, Pedivellano, Royer, and Pellegrino (2020) and Madonna (2021).

odic orbits relative to each other in order to not obstruct other space segments (Goel, Lee, & Pellegrino, 2017). Algorithms to optimize such relative movements within the constellation are also being developed (Goel, Chung, & Pellegrino, 2017).

#### 2.4.2. Helical arrays

As briefly mentioned before, the CASSIOPeiA concept is pursuing a very different solution to avoid the power-optimal guidance problem. By maintaining the underlying concept of sandwich modules but arranging them along a double-helical structure around a central axis instead of in a planar fashion, a continuous duty cycle in GEO could be achieved without sudden attitude adjustments (Cash, 2021a). As a result of the change in satellite design, L-shaped sandwich module variants as shown in figure 5 are employed, with PV and RF components placed on a common substrate on the horizontal plane. The other branch of the L would mostly consist of smaller struts to connect to the adjacent horizontal layers as well as lenses and secondary reflectors. The antennas would be spaced on the substrate in consideration of the employed wavelength.

As introduced in section 1.2, the helix would be complemented by two solid state-symmetrical reflectors on each end (Cash, 2019). The dual primary reflectors above and below the orbital plane would be sun-referenced and focus the light onto the helix. By collimating the sunlight, they would ensure uniform lighting of the sandwich array. Additional secondary reflectors integrated into the sandwich modules would then re-collimate the rays onto the PV chips. While the current module design for CASSIOPeiA is planning on using standard III-V multijunction space cells with on-chip concentration, the technologies discussed in section 2.2 could theoretically also be applied to further optimise for weight, power, efficiencies, and radiation resistance. Given that the aperture of a helix is constant from every angle, the structure itself can furthermore intercept an equal amount of sunlight from every side. However, since the reflectors providing the first step of concentration are static, the satellite has one pre-

ferred orientation towards the sun (Cash, 2021b). Therefore, the structure will have to rotate while orbiting to ensure the side which maximises light collection is always directed towards the sun.

So far, we seem to be facing a similar problem with the helical array as with the planar array. With the orientation relative to the sun remaining constant, the orientation towards the receiving station on earth is perpetually changing. However, superior flexibility of the antenna function integrated into the helical array aims to tackle this issue. Each of the L-shaped sandwich modules would be comprised of three flexible dipole antennas forming one antenna element which can be associated with one or multiple PV devices on a common substrate (Cash, 2021b). By strategically placing these three flexible dipole antennas on each sandwich module, omnidirectionality for the microwave beam can be achieved. The projected area of the helix remaining constant from every angle also means that the surface area of the transmitting aperture facing the rectenna will technically remain constant despite the rotation (Cash, 2017). All antennas would then be connected to a system-wide synchronized timing reference source to manage the 360-degree steering capabilities of the antenna array through phase shifting of the individual signals. This is discussed in more detail in the following section. Overall, the structure can therefore slowly gyrate to maintain optimal orientation towards the sun while continuously transmitting to a fixed point on earth due to its collective 360-degree steering window. As we have seen, the resulting continuously available mass-specific RF power of 1.51 W/g can be considered very competitive.

Despite these clear theoretical advantages, which have yet to be confirmed through a prototype, some drawbacks remain. Due to the increased complexity of the structure, it is not as easily scalable as planar arrays. To increase the power capacity in space, an entire new satellite would have to be launched each time instead of just adding parts to the existing one. Due to the use of sandwich modules, a certain portion of modularity is still maintained, which will be beneficial for

manufacturing and repairs. Similarly to the deployment of the planar variants, the nominally 1.7-km tall core structure of the helical array would be collapsible and enable automatic unfolding with the help of springs and releases (Cash, 2021b). The targeted dimensions for the packaged helix have not been disclosed yet. However, autonomous space robots are anticipated to conduct some of the in-orbit assembly. This issue is briefly discussed in section 4.2.

## 2.5. Array management

Essentially, array management fills a critical role as enabler of the modular sandwich structure. The benefits of modularity for SBSP systems inevitably result in the antenna being broken up into multiple smaller transmission devices. In this section we discuss how an array comprised of a large number of individual antenna elements can still act like one big antenna by exploiting some of the basic characteristics of waves. While such an approach may come with a number of advantages compared to a singular big antenna, it also poses some technical hurdles. This is particularly true for structures as large as the ones required for SBSP. As the coordination between the modules requires some form of connection, often in the form of cabling, it would add complexity and weight to the space segment. However, there are some new approaches that aim to overcome this. Nonetheless, the underlying concept is rather intuitive and essentially does not differ between planar and helical arrays.

### 2.5.1. Phased arrays

Generally, forming a continuous microwave beam carrying large amounts of energy over long distances is challenging. As a result, microwave power sources exceeding 10 kW are typically pulsed as devices capable of continuous transmission are rare, expensive, and difficult to maintain (Rodenbeck et al., 2021). All these characteristics make them ill-suited for SBSP. Instead, multiple smaller apertures arranged on a common surface can send out beams with lower power in a concerted fashion, which then reach their target as if they were a single high-power signal.

However, this set-up requires extensive coordination between the individual elements regarding targeting, amplitude, and phase alignment. Synchronization is therefore critical, for which a common low-frequency reference signal is typically employed across the entire system. Phase shifting devices integrated into the antenna elements can then select appropriate shifts for each transmission device to adjust the beam dimensions for a given task. Beam formation then happens by exploiting constructive and destructive interference between the respective electromagnetic waves. Varying phase shifts and amplitudes also allows the direction of the beam to be controlled, which is typically constrained to a 45-degree window if the antenna surface is planar (Cash, 2021b).

Besides enabling the use of sandwich modules, there are a number of benefits to this power transmission approach. Spatially combining smaller microwave sources offers great

scalability in power and distance, which can be tailored for every specific application (Gal-Katziri & Hajimiri, 2018). Additionally, such arrays offer greater beam steering capabilities, added directivity, and enhanced signal-to-interference and signal-to-noise ratios, which also scale with the number of array elements (Stutzman & Thiele, 2012).

So far, phased arrays are already used in radar, sensing, and communication systems (Gal-Katziri & Hajimiri, 2018) but not yet at the kilometer-scale envisioned for SBSP. Typically, they are also bulky, rigid, and heavy (Hashemi et al., 2019). All these qualities would be major disadvantages in SBSP. Hence, there have been first attempts to create large-scale flexible array systems. Experiments using a 16-element  $4 \times 4$  array powered by integrated geometric concentrator PV cells while operating at around 10 GHz and with an aerial density of  $1,000 \text{ g/m}^2$  have been able to successfully power a small LED over a very short distance (Hashemi et al., 2019).

Another potential benefit of light-weight flexible arrays is the possibility of lensing, specifically for planar arrays. Through a combination of the right architectures, circuits, and algorithms, dynamic 3-D lensing of the flexible phased array can result in a higher degree of focus of the microwaves. First tests using free-space dynamic lensing have succeeded in focusing and refocusing of the electromagnetic power beaming field at a distance (A. Hajimiri, Abiri, Bohn, Gal-Katziri, & Manohara, 2020). Using this technique, any field profile permissible by the laws of physics could be created through the correct setting being applied to the individual elements. This could include beam distributions that either form a focal point or maximize the total recovered power at an unknown location in the near or far field. Crucially, the array used for lensing can be arbitrary and non-uniform. This would be very advantageous to the scalability of planar arrays as their shape can vary when elements are added. However, lensing would alter the attitude of the solar side of the array in a non-uniform fashion, the potential effects of which have not yet been investigated.

### 2.5.2. Optically scanned arrays

So far, the coordination between the antenna array elements has mostly been achieved electronically. The common reference signal is therefore distributed to the modules via cables. These so-called Active Electronically Scanned Arrays (AESAs) are still in active development today for RADAR applications (Yeary, Palmer, Fulton, Salazar, & Sigmarsson, 2021). However, with large arrays such as the ones required for SBSP, electrical synchronization can become challenging. Especially with the shift to more lightweight and thin-film functional elements, the infrastructure for synchronization starts to become one of the main drivers of system cost, mass, and power consumption (Gal-Katziri, Ives, Khakpour, & Hajimiri, 2022). Maintaining timing accuracy for the reference system across a large array electronically also remains a major challenge (Gal-Katziri & Hajimiri, 2018). Hence, electric synchronization mechanisms do not scale well with the array size.

Researchers are therefore looking to replace electronic interfaces with optical connections. The addition of an on-chip photodiode would allow for the timing information to be distributed over long distances via an optical carrier (Gal-Katziri et al., 2022). This optical carrier could either move through fibre or free space. Unlike electric cables, especially the latter option is characterised by great physical flexibility, enhancing modularity and all its benefits. Another benefit would be a reduction of losses within the synchronization infrastructure. For very large arrays, such as a space solar power station, it would also be possible to mix optical synchronization with local electrical synchronization. Overall, optical timing synchronization could therefore be a viable alternative or addition to standard electronic modalities for SBSP by enabling large, scalable, cheap, and lightweight phased array applications. The elimination of cabling could also prove another boost to weight-specific power metrics. Optical information transfer has further been shown to be interoperable with the lensing of flexible arrays (A. Hajimiri et al., 2020).

### 2.5.3. Phased array algorithms

Lastly, phased arrays need the right algorithm to optimize beam formation and steering. These algorithms need to be adaptive and respond quickly when, for instance, small deformations due to microgravity threaten to exceed the very limited beam steering tolerance from GEO of 0.0005 degrees (ITU, 2021a). Development of such software suitable for SBSP has been progressing recently.

In 2020, the previously 16-element flexible phased array at 10 GHz has been enlarged to 256 elements (Gal-Katziri et al., 2020). By employing a specifically developed algorithm, researchers successfully demonstrated 2-D beam-steering and correction capabilities in response to deformations. The algorithm was also able to focus the beam of a 400-element device and concentrate power on a receiver whose location was previously unknown to the computer. For helical arrays, an additional variable would enter into the algorithm in the form of which of the three dipole antennas of a module should be activated, based on the relative position of the target. Otherwise, the concept remains largely the same.

### 2.6. Orbits and constellations

With the help of reflectors, a SBSP satellite can achieve 100% duty cycle in GEO by keeping its transmission array earth-oriented. The reflectors then ensure that the solar side of the panels is evenly illuminated, no matter their relative position to the sun. Staying in GEO also ensures that earth does not throw a shadow upon the satellite at any point during the rotation. Such characteristics make it the orbit of choice for all our selected SBSP concepts. However, obtaining GEO requires the satellite components to cover over 35,000 km. Such a great distance results in higher launch costs than closer orbits, which is discussed in more detail in section 4.3. Additionally, as investigated in the following chapter, the greater the distance the larger the microwave transmit and receiver apertures need to be to obtain sufficient

efficiencies. Lastly, due to its unique and desirable properties, GEO has already been considered as crowded for a number of years (Jehn, Agapov, & Hernández, 2005). Consequently, researchers have started to look at alternatives that alleviate those problems while maintaining as high of a duty cycle as possible to limit LCOE.

Generally, when a single SBSP satellite moves closer to earth, its duty cycle decreases as the eclipse duration increases and the structure will no longer be stationary relative to the rectenna. As a result, the squint angles required to keep the satellite transmitting for as long as possible increase. Therefore, a single SBSP satellite in a lower orbit than GEO would again be subject to intermittency, potentially requiring grid-scale storage at the ground station. We are therefore facing a trade-off between accessibility, costs, and continuous power supply.

The intermittency issue for closer orbits could be partially overcome by employing a constellation of SBSP satellites. This would ensure that at any point in time, there is a satellite available that is outside the local eclipse and within the maximum permissible squint angle window of the transmit and receiver apertures. MEO would then be the preferred option as configurations would be possible where the individual pass time is still long enough that only few additional satellites would have to be put into operation (Marshall et al., 2021). This is particularly important seeing that multiple space segments would also require more launches. However, MEO also suffers from a much harsher radiation environment than GEO (Larson & Wertz, 1992), increasing the importance of some of the inherently radiation resistant technologies discussed above.

Overall, constellations in MEO consisting of four smaller satellites or more to reduce elevation angles and ground station size while maximising the overall duty cycle can be cost competitive with system in GEO (Marshall et al., 2021). The power-optimal guidance problem from Marshall et al. (2020) could then be extended to N separate space vehicles. Despite multiple satellites also requiring more launch capacity, an issue discussed in section 4.3, they might ultimately be more feasible given the far greater amount of orbits available in MEO.

Furthermore, for planar arrays without external reflectors, the benefit of using dual-sided over single-sided sandwich tiles diminishes as the orbit is decreased and the amount of satellites increased (Marshall et al., 2020). This dynamic is based on the fact that now not a single satellite alone determines the overall duty cycle. Instead a single satellite in position is enough to continue supplying energy to the grid. As a result, satellites could also be smaller while in total providing the same amount of energy. A single satellite at 2 W/g but with a duty cycle of only 50% would, all things equal, provide the same energy as a constellation of smaller satellites with 1 W/g each operating at an overall duty cycle of 100%. Additionally, a constellation could provide power to multiple rectennas on earth simultaneously, given they are spread out enough. This idea is further being pursued as one option for the CASSIOPeiA project to allow for better collaboration

between different governments.

Lastly, as the orbit decreases and the amount of satellites increases, the share of LCOE attributable to the space segment grows (Madonna, 2018). Consequently, the critical metrics for the space segment defined in this chapter become even more important for overall system economics. With the larger squint angles at lower orbits, the required size of the rectenna would also increase. However, this additional cost is insignificant in comparison to the space segment.

## 2.7. Conclusion

Overall, a number of technology approaches were introduced which are currently not factored into some of the most developed SBSP concepts. Table 1 allows us to directly compare radiation benefits and conversion efficiencies as well as mass-specific power and aerial density values for different parts of the satellite. As explained initially, some numbers from the literature had to be adjusted or extrapolated upon to achieve a like-for-like comparison. In the table, these are shaded in violet. We will begin by summarising the assumptions and the basis upon which they were made. Extensive explanations and references are also provided in the model that was used for the calculations.

To obtain an estimate of the metrics if a new solar technology were to be implemented into a lightweight sandwich module and vice versa, we have calculated a weight premium of 29 g/m<sup>2</sup> which accounts for DC-to-RF and antenna layers. This weight premium is based on an average of the masses reported in Warmann et al. (2020). For dual-sided module designs, a factor of 1.3 was applied to account for shared infrastructure and the mesh design of the optically transparent RF components. An additional weight premium of 32 g/m<sup>2</sup> based on Gdouts et al. (2020) was used to simulate the effect of supporting and deployment structures for when the sandwich module is integrated into a planar array. Given that we apply the same premia to all technology options, we maintain comparability.

The assumed DC-to-RF efficiency of 70% sits at the lower bound of the investigated concepts and assumptions in the literature (e.g. Sasaki, Tanaka, & Maki, 2013). Furthermore, it is in line with what has been achieved during recent demonstrations for tube-based (Mihara et al., 2018) and semiconductor amplifiers (L.-C. Zhang & Shi, 2022).

When comparing the space segments of the selected concepts, CASSIOPeiA achieves the highest specific power at the lowest overall aerial density. One potential reason for this could be the consequential use of light-weight sandwich modules and high solar concentration levels. In particular, it compares favourably to SPS-ALPHA, whose numbers appear to remain subdued based on heavy module components and external reflector structures. The only concept not employing sandwich modules is MR-SPS, which consequently reports the lowest specific power numbers although not the highest aerial density. The lack of any solar concentration further limits power output. In conclusion, all but CASSIOPeiA fail to beat the baseline comparison CIC and flat-plate cells once transmission infrastructure or more is added. The fact

that SPS-ALPHA has a lower  $p_{PV}$  than the mass-optimised flat-plate cell despite employing concentrators is likely attributable to the weight of its reflector structures.

Consequently, lightweight concentrator alternatives would be needed. While integrated parabolic mirror modules achieve the highest specific power across all options, in part due to their ultralight design, the lack of commercial availability for the CFRP materials and the complicated production makes their employment at scale uncertain. LSCs could prove to be a viable alternative. However, so far their low PV efficiencies limit specific power results. With convergence of efficiencies, they could become the solar concentration technology of choice due to their low weight, flat-plate geometry, and unconstrained acceptance angles in addition to enhanced radiation resistance.

On the materials side, perovskite has established itself as one of the elements displaying some of the highest  $p_{PV}$  values when used in a solar cell. This is despite its PV conversion efficiency only reaching about half that of more established alternatives. Even without any further light concentration, our calculations suggest that it would be able to provide significantly more than 1 W/g, even when integrated into a full array. Its self-healing properties after radiation damage also makes it well suited for the harsh environments of space, particularly when moving from GEO to MEO. Radiation resistance and the resulting weight reduction when other protective measures are removed is also the chief advantage of cells based on nanowire technology. Therefore, nanowires might offer an opportunity to radiation-proof the peripheral components to a perovskite cell and should therefore be used in conjunction with any other radiation-proofing technologies.

Lastly, when comparing our heuristic calculations on dual-sided sandwich modules, it seems that the additional weight would not be too detrimental to their performance. Mass-specific power values fell by about 20%. Therefore, a commensurate boost to their duty cycle would be required to keep mass-specific energy constant. Given that initial studies suggest an increase of 50% to the duty cycle when a second RF layer is introduced, the result would be net positive. Our simulated planar arrays containing these modules also perform at or above the levels of SPS-ALPHA or MR-SPS. However, they are still very early in their development and further tests will have to be undertaken to determine whether such changes to the module are the right approach to solving the power-optimal guidance problem of planar arrays. As a structural alternative, helical designs also come with their own trade-off between a continuous duty cycle and additional weight as well as reduced modularity, flexibility, and scalability. Both helical and planar arrays could then benefit from further mass reductions through at least partially optically synchronised arrays.

In conclusion, the technology alternatives investigated are not exclusively applicable to only one type of satellite. Their utilization in practice should therefore not depend on whether planar or helical structures are ultimately employed. Arguably, all of the concepts might be improved by employing a combination of new technologies. Based on our results, in-

**Table 1:** A comparison of mass-specific power and aerial density calculations between established satellite concepts and technology alternatives suggests that some innovations could offer notable improvements. Shaded cells indicate that adjustments or extrapolations based on the literature were necessary to obtain a like-for-like comparison. Further indication is given whether a certain technology uses solar concentration or offers radiation resistance. Based on own calculations using the numbers reported in this chapter.

		Solar concentration	Radiation resistance	Conversion efficiency		Specific power [W/g]			Aerial density [g/m <sup>2</sup> ]		
				PV* -to-DC	DC:RF	PV*	PV* + RF	Satellite	PV*	PV* + RF	Satellite
Concepts	SPS-ALPHA	X		48%	71%	0.95	0.33	0.32	1,598	3,222	3,393
	CASSIOPeiA	X		31%	85%	2.51	1.51	1.51	491	692	692
	MR-SPS <sup>†</sup>			25%	83%	1.20	0.27	0.16	333	884	1,474
Baseline	CIC			32%	70%	0.54	0.36	0.35	804	833	865
	Mass-optimised flat-plate cell			34%	70%	1.00	0.67	0.62	450	476	508
Integrated parabolic mirrors	7.5 suns low emissivity	X		32%	70%	3.75	2.10	1.72	116	145	177
	15 suns low emissivity	X		32%	70%	5.20	2.59	2.02	83	115	147
	15 suns low reflectivity	X		29%	70%	5.90	2.87	2.15	67	96	128
LSC	Standard	X	X	12%	70%	1.16	0.67	0.57	140	169	201
	Bandwidth optimized	X	X	18%	70%	1.84	1.07	0.90	140	169	201
Cell	Perovskite		X	15%	70%	29.40	2.49	1.26	4	33	65
Nanowire	CIC w/o cover glass		X	32%	70%	1.56	0.99	0.89	278	307	339
	Flat-plate cell w/o cover glass		X	34%	70%	3.00	1.76	1.49	150	179	211
Dual-sided sandwich	CIC with dual-sided RF			32%	70%	0.54	0.28	0.27	804	842	874
	Flat-plate cell with dual-sided RF			34%	70%	1.00	0.51	0.48	450	488	520

\* PV includes reflector/concentrator arrays and structures directly attributable to them  
<sup>†</sup> Not based on sandwich module design  
 Adjusted or extrapolated metric

corporating LSCs into perovskite nanowire cells could result in significant weight reductions, increased inherent radiation resistance enhancing operational lifespan, and notably improved specific power as well as aerial density metrics. These elements could then be incorporated in a sandwich module, given their superior performance when compared to the Chinese variant with separated surfaces. The sandwich modules could then either be used in a planar or helical array and therefore improve the SPS-ALPHA and CASSIOPeiA concept alike. All these optimisation consideration become an even bigger lever for overall system economics if multiple satellites are employed in a lower orbit as their share in LCOE increases markedly.

### 3. Wireless power transfer and ground structure

Today, we transport energy by various means. Primary energy in the form of oil and gas is hauled across oceans

and continents via ships and pipelines. Cables conduct electricity through buildings around the country and under the sea over large distances, connecting grids around the world. WPT follows the same concept of moving energy from point A to point B - just without any physical structures in between. Therefore, a concrete use case might be that point B is a place to which energy is difficult to get to and far away from point A, where energy is abundant, with the area between being ill-suited for wires. This concept also underlies its application to SBSP

Generally, WPT is defined as "the efficient point-to point transfer of electrical energy across free space by a directive electromagnetic beam" (Rodenbeck et al., 2021) and therefore, in contrast to passive energy harvesting applications, pursues the maximisation of total power transfer efficiency. A standard set-up consists of a transmitting aperture which converts DC power to the electromagnetic waves of choice and which are then sent to a receiving aperture a set distance

away to convert the waves back to DC power.

While the focus of our analysis of WPT remains on its specific applications to SBSP, there is also ongoing research into the idea of energy harvesting, which collects ambient energy present in the form of microwaves to generate electricity (Kazmierski & Beeby, 2014). WPT is also classified as an enabling technology for 6G (Saad, Bennis, & Chen, 2019). Furthermore, we will see in section 3.3.1 that the military has played a critical role in fuelling research behind WPT and continues to do so today, particularly in the United States. While the military always has an inherent interest in space, the strong association of the defence sector with SBSP could pose geopolitical hurdles for its adoption. SBSP satellites could be used to power remote military bases and vehicles (Masrur & Cox, 2019). Theoretically, militaristic applications could also extend to the delivery of disruptive or even destructive electromagnetic power against targets on earth or in space. Therefore, SBSP could be a topic of interest for the UN Committee on the Peaceful Uses of Outer Space to generate operational consensus across nations. These considerations, however, are outside the scope of this thesis.

### 3.1. Metrics for power beaming evaluation

The following three metrics have been identified from the literature (e.g. Rodenbeck et al., 2022) as key determinants of power beaming systems with a primary focus on microwave power beaming:

#### *Link efficiency [%]:*

Link efficiency is often used to describe the share of DC power that is ultimately available at the ground structure after conversion to RF or laser, transmission to earth, collection, and reconversion. Therefore, it is comprised of a collection of efficiencies corresponding to each of these steps. While in theory it would be possible to break the conversion chain down to each individual hardware component, we focus on the sub-efficiencies commonly reported in the literature on WPT demonstrations. This leaves us with three main efficiency metrics for microwaves. First, DC-to-RF efficiency typically includes losses incurred from routing DC power around the space segment and the efficiency of the transmitting antenna. Next, collection efficiency measures the share of emitted electromagnetic waves that ultimately impinges on the reception area of the rectenna. Transmission losses due to interference with the weather and atmosphere are also often included in this metric. At the rectenna, RF-to-DC efficiency is simply the rectification efficiency, including the routing of DC power around the rectenna. For laser beaming, the final step would entail optical-to-DC reconversion via specialised PV arrays. The DC-to-AC conversion required to feed the generated electricity into the grid is not included in any demonstrations but is a standard procedure with relatively high efficiencies.

#### *Frequency [GHz]:*

The frequency at which the beam is sent out does not per se determine system performance. However, the chosen frequency has significant implications on overall system design,

the scale of the apertures, as well as interactions with the environment. Therefore, it is an important metric when comparing power beaming systems. For optical transmission systems, the wavelength measured in nanometres, which can be easily derived from the frequency, would be the more commonly used metric.

#### *Power density [ $W/m^2$ ]:*

The power density measures how much power is successfully transferred and collected per unit surface area of the receiver aperture. As beams will not be uniform in their power distribution across the surface area, even with proper focussing, a distinction can be made between the average power density across the entire structure and the peak power density incurring only at certain points. The average density is mostly important to the scale of the ground system while the peak density is of particular importance for safety considerations and certification. It can also be expected that power densities will be an important cornerstone in public discussions to build social acceptance, given their close link to system safety.

Regarding the evaluation of demonstrations, it is important to note that inconsistencies in the reported efficiencies of power beaming demonstrations are common (Rodenbeck et al., 2021). Not always are the system boundaries clearly defined and hence some numbers might not be directly comparable. Sometimes certain metrics are omitted completely from the publication. There are some older meta studies that constitute notable exceptions (Brown & Eves, 1992). For future research efforts, it will be crucial that parameter reporting is as uniform as possible with clear definitions of the system boundaries and corresponding hardware components. Additionally, more holistic metrics for evaluation, which may also include costs, have been proposed in the past but not caught on (Dickinson & Maynard, 1999). Nonetheless, efficiencies without such a clear framework, as most of the ones reported in the past, are still helpful to obtain a general understanding of the maturity and progress of microwave power transmission (MPT) or laser power transmission (LPT) technologies.

### 3.2. Beam types and atmospheric attenuation

The three main types of electromagnetic beams which have been examined for the purpose of power beaming are optical lasers, millimetre waves (mmWaves), and microwaves. Microwaves generally have a frequency ranging from 300 MHz to 300 GHz, whereas mmWaves are a subset of microwaves, representing the higher end of the spectrum at 30 to 300 GHz. On the other hand, laser frequencies are multiple orders of magnitude greater and measured in THz.

For the purpose of SBSP in GEO, these beams have to transport large quantities of energy over distances exceeding 35.000 km. While the majority of their journey will lead them through the vacuum of space, the electromagnetic waves will ultimately also encounter the earth's atmosphere. Here, any beam will experience losses due to interference by the molecules along its path. Coming from GEO, the smallest number of interactions would take place with a receiver

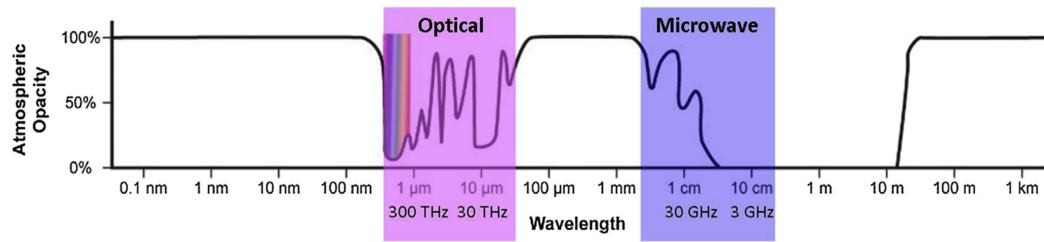


**Figure 8:** Opacity windows in the atmosphere for optical waves and microwaves. (Jaffe, 2020)

placed directly at the equator, constituting an air mass coefficient of one (AM1). However, the further you move away from the equator, the more atmosphere the beam will have to cross and the more losses it will therefore accrue.

The magnitude of these losses is also closely tied to the wavelength of the beam. Consequently, it is not the entire frequency range of light and microwaves that is relevant to WPT. One of the factors determining the bands of interest are the opacity windows in the atmosphere. These windows represent wavelengths or frequencies where interactions are minimal and are represented in figure 8.

Consequently, to minimise atmospheric losses, frequencies towards the lower end of the microwave band should be deployed, with opportunities for mmWave applications in the  $K_a$ - (26.5-40 GHz) or W-band (75-110 GHz). The latter two are highlighted in green in figure 9. These environmental circumstances are further reflected by the fact that the frequencies considered for SBSP are 2.45 GHz and 5.8 GHz (ITU, 2021a). Most demonstrations have employed these levels as well, as we will see in section 3.3.1. In these frequency ranges, atmospheric losses are very small, which makes them well suited for SBSP applications (ITU, 2019).

Converseley, optical applications should use the visible or near infrared parts of the spectrum to utilize the atmosphere's opacity windows. However, energy densities of lasers are by some orders of magnitude higher compared to microwaves (Grandidier et al., 2021), resulting in higher atmospheric losses overall and also poor weather penetration characteristics.

Impediment by weather is another factor of importance when comparing modalities of WPT. While microwave transmission has fewer problems with this as seen in figure 9, lasers tend to be constrained in rainy or foggy conditions. Such issues have also already been observed with other laser applications such as LIDAR (Heinzler, Schindler, Seekircher, Ritter, & Stork, 2019). This presents difficulties for SBSP given how the underlying concept of renewable baseload power requires the satellite to transmit energy at any time, especially during extreme weather events.

A comparison of all characteristics with respect to the three modalities, including atmospheric penetration, is synthesized in table 2. Overall, one of the chief benefits of optical WPT is the small aperture size. However, despite decent conversion efficiencies, the poor penetration characteristics paired with more stringent safety requirements also resulting

from higher power densities present difficulties for SBSP applications. Crucially, optical transmitters at current technological levels are also very difficult to scale due to mechanical tolerances and costs. mmWave applications also suffer from this limitation, despite displaying potentially enhanced safety characteristics, as has been shown in recent demonstrations (Rodenbeck et al., 2021). Nonetheless, this makes these two modalities less suited for the long distances required by SBSP concepts.

In comparison, systems based on microwaves not only perform well on the atmospheric front but also scale in power proportionately to the aperture areas, which constitutes a relatively easy way to enhance system performance. Furthermore, progress in the past decade with vacuum and solid state amplifiers in the antenna allows for higher DC-to-DC conversion efficiencies (Grebennikov, 2011). However, it should be noted that, compared to mmWaves, microwave frequencies correspond to bigger wavelengths, making it very difficult to integrate entire antennas on-chip as has been achieved for mmWave applications (Shaulov, Jameson, & Socher, 2017).

Overall, microwave systems have been favoured for WPT, as evident in the many decades of demonstrations since the middle of the 20<sup>th</sup> century. Next, we briefly discuss microwave WPT and some of the most significant demonstrations. Nonetheless, we will also briefly show some experiments based on laser transmission and safety-enhancing technologies in section 3.4, as notable progress could be observed in recent years.

### 3.3. Microwave power beaming

In this section, we start with a brief look at the physical dynamics of WPT systems based on microwaves. Then we will highlight important steps in the history of microwave power beaming, including past and recent demonstrations, followed by spectrum and safety management.

A system to transmit power from a solar satellite in GEO via microwaves would see the generated DC electricity converted to microwaves and send out in form of a beam via an antenna array connected to the orbiting body. As discussed in section 2.5, this transmitting array needs to be phase-calibrated to achieve a concentrated beam for maximum efficiency and targeting precision. The optimal power distribution for a transmit would then roughly resemble the Gaussian curve (Brown & Eves, 1992). The receiving site would convert microwaves to DC using a rectifying antenna (rectenna).

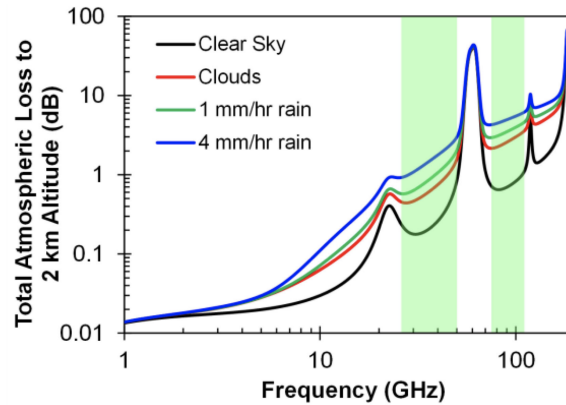


**Figure 9:** Attenuation effects of different weather scenarios on microwave frequencies. (Rodenbeck et al., 2021)

This rectenna combines an antenna for collection, input filters, rectifying diodes, and an output filter to ultimately feed electricity into the grid (Brown, 1977). Modern versions of such a receiver can take the form of a mesh-like structure. As a result, there are deliberations that a rectenna could be combined with other renewable sources such as terrestrial solar and wind or even employed on agricultural land (Jaffe, 2020).

Integrated rectenna approaches might help with social acceptance, given that the structures would have to be quite large to be efficient. This relationship between size, wavelength, and efficiency for the purpose of SBSP WPT has been expressed by Shinohara (2014), amongst others, via the following formulas.  $A_t$  and  $A_r$  denominate the area of the transmitter and receiver apertures, respectively,  $D$  the distance between the two, and  $\lambda$  the transmission wavelength.

$$\tau^2 = \frac{A_t A_r}{(\lambda D)^2} \quad (12)$$

$$\eta_{Link} = \frac{P_r}{P_t} = 1 - e^{-\tau^2} \quad (13)$$

The metric  $\tau$  relates these parameters in a way that allows to model link efficiency with the help of equation 13. Both formulas are an adaptation of the Friis transmission equation. Changes are necessary as the Friis variant relies on far-field assumptions that do not apply to WPT (Shinohara, 2014). The far field parameters used for more standard RADAR applications typically do not focus on finite distances. However, maximum energy transfer happens in the radiative near field or Fresnel region, which can still translate to long absolute distances for smaller wavelengths (A. Hajimiri et al., 2020).

The adapted equation demonstrates the trade-off at the core of the system between utility due to size and efficiency. One driver of this dynamic is the collection efficiency, which is the proportion of the radiated waves that ultimately meet the rectenna surface. Any waves that do not reach the receptor result in power being lost. Diffraction physics lead

to the simple conclusion that the waves will always be scattered to some degree, requiring very large receiver sizes for the distances encountered with SBSP. Equation 13 does not take these sidelobes into account but could be tweaked by including the beam pattern (Shinohara, 2014).

For an example calculation, a SBSP system in GEO with a 1-km transmit aperture as well as a rectenna measuring 3.5 km in diameter operating at 5.8 GHz could theoretically reach a 90% collection efficiency. It has also been shown that collection efficiencies close to 100% are achievable in practice but require diligent alignment as well as optimised amplitude and phase distributions (Brown, 1974). An even larger transmit array or rectenna could theoretically, within limits, improve this number further. Additionally, should the rectenna not be placed at or near the equator, its required shape would shift to elliptical due to the resulting higher elevation angles of the beam and its surface area would increase further.

On the other hand, the inverse also follows from the equation. As opposed to having large structures in GEO and on the ground to achieve high beam efficiency over long distances, a closer orbit would allow for smaller apertures. However, lower orbits such as MEO would also present two big drawbacks. First, the transmitting and receiving areas would now move relative to each other as the geostationary properties are lost. Hence, some kind of guidance system would be required to maintain the link within the steering tolerance of around 0.0005 degrees (ITU, 2021a). The solution that has been devised to overcome this issue are pilot signals. These are sent from the rectenna to the transmit array and have proven safe and effective (McSpadden & Mankins, 2002). The CASSIOPEIA concept, for example, also plans to employ an encrypted pilot beam to maintain connection for its 1 to 10 GHz WPT system. We will further discuss pilot signals later on. The second drawback is the loss of constant coverage due to relative positioning and effects of earth's shadow. As a result, a single SBSP satellite would no longer be able to provide renewable base-load power continuously. However, a constellation of multiple satellites can overcome this

**Table 2:** Comparison of the three beaming modalities. Microwaves appear best suited for high-power long-distance applications such as SBSP. Own adaptation based on Rodenbeck et al. (2021)

	Optical	mmWave	Microwave
<b>Weather penetration</b>			
Clouds/rain/fog	No	Poor	Very good
<b>Conversion efficiency</b>			
Performance limits for DC/RF conversion	OK	OK	Good
<b>Required aperture size</b>			
Transmitter/receiver aperture sizes	Small	Medium	Large
<b>Safety</b>			
Required due regard, pointing, user perception	OK	Good	Good
<b>Economy of scale</b>			
Present capabilities for high-power/long-distance	Poor	Poor	Good

challenge as discussed in section 2.6.

One factor that has hampered demonstration results from the very beginning until today are the hardware components. Similar limitations such as seen with the Friis equation and underlying far-field assumptions also apply to some of the standard RADAR components used in most WPT experiments. As they are not optimized for high-power beam transmission and collection efficiency at range, achieved link efficiencies can be limited (Shinohara, 2014). One way around this would be customized equipment as used by William Brown during his infamous JPL demonstration, which we will elaborate on shortly.

Overall, there are many trade-offs and challenges when it comes to WPT for SBSP applications. Nonetheless, over the past decades there have been a number of successful demonstrations of the underlying technology using microwaves. In the following section, we briefly introduce the developments and people that led to these achievements, paving the way for today's experiments.

### 3.3.1. Overview of power beaming demonstrations

In this section we introduce a summary of past, present, and planned microwave power beaming demonstrations and what kind of results they were able to achieve. A generalized representation of a power beaming demonstration, including the key metrics, is provided in figure 10.

#### Early history

After the concept of transporting electricity in a vacuum without wires was theorised by James Maxwell in 1873 and later theoretically validated by Heinrich Herz around 1890, Nikola Tesla conducted the first experiment with WPT around the turn of the century (Tesla, 1904). Sending alternating surges through masts and thus creating a standing wave between them, he then placed receiving antennas at maximum amplitude points. However, this failed to achieve any significant power transfer (Cheney, 1981). After this unsuccessful demonstration, momentum died down until the middle of the 20<sup>th</sup> century.

#### U.S. dominance

With the resurgence of interest in RADAR technology during the second world war, the idea of the wireless transfer of electricity using microwaves also intrigued the military. Further inspired by Isaac Asimov's short story "Reason", which we already introduced in section 1.1 as the first description of SBSP using WPT, the U.S. defense sector started looking into the concept.

At first, focus remained on the possibility of using WPT to power unmanned aircraft for surveillance and communication purposes. In 1959, the defence contractor Raytheon proposed the Raytheon Airborne Microwave Platform (RAMP). The idea was to deploy a small helicopter at 15 km altitude which would act as a communications node and be powered by microwaves from the ground. The required amplatron with an output of 400 kW at 3 GHz and a transmitting efficiency of about 80% was then developed by Raytheon's scientist William Brown in the following year (Skowron, MacMaster, & Brown, 1964). This project marked the beginning of the golden age of WPT demonstrations as well as Brown's position as a pioneer in the field. Shortly after, NASA, who was also involved, successfully improved some key components of the beaming system, allowing for more concentrated beams and hence higher collection efficiencies (Potter, 1961).

In 1963, Brown went on to develop the first complete modern WPT system at Raytheon's lab. The set-up used a magnetron coupled with a reflector to send microwave energy at 3 GHz over a distance of 5.5 m. The resulting DC-to-DC conversion efficiency came in at 16%, based on an 87% collection efficiency and a 50% rectifier efficiency with 100 W of output (Brown, 1980a). Another key element to this experiment was the first modern rectifying antenna to receive the microwaves and convert them back to DC power. Brown was helped by fellow researcher Roscoe George in developing this aperture. Together, they patented the rectenna design a couple of years later (Brown, George, Heenan, & Wonson, 1969). George also conducted his own demonstrations at Purdue based on the design but only managed to achieve 40% RF-to-DC conversion efficiency (George & Okress, 1968). Spurred on by the initial success, addi-

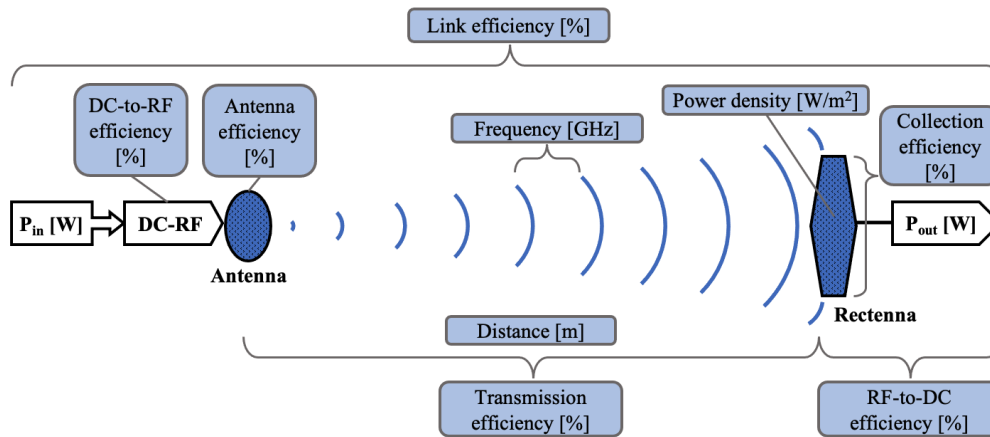


**Figure 10:** Visualisation of a general power beaming demonstration using microwaves, including the key reported metrics relevant to our analysis. The antenna and rectenna can either be stationary or affixed to moving objects such as terrestrial or aerial vehicles. Own representation

tional contracts were given out to pursue the RAMP concept. Consequently, in October 1964 Brown conducted the first microwave-powered small aircraft flight for which a small helicopter was flown at an altitude of 15.2 m for the duration of 10 hours (Brown, 1965).

Towards the end of the 60s, attention also started shifting towards the possibilities of power beaming in space. Intrigued by Peter Glaser's first concept for SBSP at Arthur D. Little in 1968 (Glaser, 1968), which he further refined in 1973 to elaborate the modalities of the power transfer (Glaser, 1973), NASA gave additional contracts to Brown to push the limits of power beaming at the time. A first demonstration at the Marshall Space Flight Center (MSFC) in 1970 resulted in a measured DC-to-DC efficiency of 26.5% (Brown, 1980a). However, one of the deficiencies uncovered by the experiment was the low rectenna collection efficiency of only 74% versus the theoretical maximum of 100%. As an improvement, the rectenna design was overhauled with elements being spaced more closely and in an overall hexagonal shape. These steps managed to push the initial number up to 93%. Furthermore, the Schottky-diodes essential to the rectification process were switched to be based on different materials. Overall, the rectenna components were also rearranged from its previously flat design to a 3-D volumetric construction to overcome difficulties arising from the new diode spacing and achieve precise polarization alignment (Dickinson, 1975). These changes also boosted performance to the point that another demonstration at the MSFC in 1974 yielded a far improved RF-to-DC efficiency of 82%, resulting in an impressive DC-to-DC efficiency of 48% (Brown, 1980a).

Activities then shifted from the MSFC to the Jet Propulsion Laboratory (JPL) and the NASA Goldstone Deep Space Communications Complex (Goldstone) in California. At this point, Richard Dickinson from the JPL also became very involved in the experiments. Ultimately, the efforts at the JPL culminated in a demonstration in 1975 where power was beamed over a distance of a couple of meters via microwaves

at 2.45 GHz, delivering DC power of 495 W at the rectenna (Dickinson & Brown, 1975). Conversion efficiencies of 69% and 79% for DC-to-RF and RF-to-DC respectively, resulted in an overall strong system efficiency of 54%. This number constitutes a benchmark that stands unbeaten to this day, despite Brown identifying technical potential to boost link efficiency further to 76% in the wake of the experiment (Brown & Eves, 1992).

Later the same year, another demonstration took place at Goldstone. Based on the improved volumetric design, the largest rectenna array to date was built, spanning 24 m<sup>2</sup> with performance still exceeding 80% efficiency (Dickinson & Brown, 1975). It was used to receive microwave energy sent from an antenna 1.54 km away at a frequency of 2.4 GHz, resulting in 30.4 kW DC power output with incident peak RF intensities of up to 170 mW/cm<sup>2</sup> (Dickinson, 1975). It remains the highest power result to date, although the end-to-end efficiency stood at only 4% as it was limited by the transmission and receiving apertures (Dickinson, 2003).

In 1976, Brown followed up his success by tweaking the rectenna design using a custom air-metal diode technology which unfortunately has since been lost (Rodenbeck et al., 2021). While its power handling capabilities were only in the 10s of watts, it helped him achieve the highest reported RF-to-DC efficiency to date of 91.4% (Brown, 1977). This result serves as an example of what could be possible with hardware customised for WPT. Nonetheless, due to the difficulties in fabrication, the 3-D volumetric rectenna design was abandoned in the 80s in favor of a thin-film variant using photolithographic techniques. The thin-film design was also able to demonstrate RF-to-DC conversion efficiencies of over 80% at 2.45 GHz (Brown & Triner, 1982).

The 1970s thus turned out to be the golden age of WPT demonstrations. The rapid progress increased NASA's confidence in the technology and its applications for SBSP. Further theoretical studies in collaboration with the U.S. Department of Energy followed, which culminated in a report concluding

that SBSP with WPT was a feasible technology for the future (Brown, 1980b). The 670-page document was also the first time the concept of retrodirectivity to keep the beam on target was introduced. However, for reasons unknown, the publication marked the conclusion of NASA-sponsored programs and hence the end of U.S. leadership in the field of WPT.

While the U.S. transitioned into a passive role, countries like Canada continued with their own research programs. The Stationary High-Altitude Relay Program (SHARP) culminated in the 20 minute long flight of a lightweight fuel-less airplane (Schlesak, Alden, & Ohno, 1985). Achieving altitudes of up to 150 m, it was remotely powered by microwaves at 2.45 GHz and power densities of up to 400 W/m<sup>2</sup> were measured at the wing. SHARP was also one of the first experiments to make use of the light-weight thin-film rectenna devised by Brown just a couple years earlier. Their properties made them particularly well suited for airborne vehicle applications.

#### *Japan's advances*

In the end, it was Japan who really took over the mantle of leadership in WPT research. As a country of few natural energy resources yet with a lot of high-tech industry, it was quickly enamoured by SBSP and its promises of some clean energy self-sufficiency. Hence, the Japanese government, universities, and businesses became quite active in the pursuit of key technologies needed for SBSP - particularly WPT. It is notable that, unlike in the U.S., the private companies came from outside the defence sector. In its pursuit, Japan continued to push the boundaries and was the first to conduct in-space experimentation in 1983. The Microwave Ionosphere Nonlinear INteraction eXperiment (MINIX) was designed to gain insights into the interactions between ionospheric plasma and high-powered microwaves (Matsumoto et al., 1982).

Another valuable contribution by Japanese researchers was the technical development of beam tracking. With the idea of retrodirectivity introduced in the 1980 U.S. report, it was scientists at Kyoto University in 1987 who collaborated with Mitsubishi Electric Corporation to develop a retrodirective transmitter for automatic beam alignment between transmitter and receiver (Matsumoto, 1989). The concept was based on the transmitting array sending the electromagnetic waves in the direction of a pilot signal operating at a different frequency. Such targeting would not only be crucial for systems operating outside of GEO, but small gravitational deformations in an array, such as introduced in section 2, could also have adverse effects on beam accuracy. The technology was then further improved upon with Nissan Motor Company in the mid 1990s.

The automatic alignment technology opened up new possibilities for experimental set-ups. In 1992 during the Microwave Lifted Airplane eXperiment (MILAX), Japan ran a successful demonstration of microwave power beaming between two moving apertures (Fujino et al., 1993). An electronically scanned phased array mounted on a moving ve-

hicle was successfully used to focus a 2.4 GHz beam on an airplane in motion relative to the ground-based aperture.

Emboldened by its quick scientific advances, Japan was then the first country to achieve power beaming in space. Its International Space Year - pulsed Microwave Energy Transmission in Space (ISY-METS) experiment on 18 February 1993 saw microwave energy beamed between two rockets during launch (Kaya, Kojima, Matsumoto, Hinada, & Akiba, 1994). One rocket was carrying microstrip antenna arrays and the other different rectennas, one of them designed in the U.S., between which microwaves were then pulsed (Akiba, Miura, Hinada, Matsumoto, & Kaya, 1993).

Additional experiments were then undertaken in the mid 1990s. The first was to better understand the dynamics of large rectenna arrays consisting of many elements and the required characteristics of each element as well as how to connect them to maximise DC output. For that reason, researchers from Kyoto University worked together with Kansai Electric Corporation to target a beam across a distance of 42 m at different rectenna constellations (Shinohara & Matsumoto, 1998). Optimal results were achieved when rectennas of equal DC output were connected. However, for the huge arrays necessary for SBSP it will be impossible to have equal microwave power densities across the entire aperture surface and very difficult to mass-manufacture elements with identical performance. We will further discuss manufacturing briefly in section 4.3. The second was another airship experiment called Energy Transmission toward High-altitude long endurance airship ExpeRiment (ETHER). A blimp equipped with a 9 m<sup>2</sup> rectenna array consisting of 1,200 elements was flown at an altitude of 50 m for four minutes (Kaya, 1996). The aircraft was powered by a microwave beam delivering 10 kW of power at 2.45 GHz. In line with most past experiments, RF-to-DC conversion efficiencies of 81% were achieved.

During the course of its MILAX and ETHER experiments, Japan also introduced dual polarization to its rectenna designs (Fujino et al., 1993). This allowed the transmitting and receiving array to be rotated relative to each other while maintaining stable DC power output. Hence, the two apertures no longer absolutely needed to be completely parallel to each other. This property would be crucial for any SBSP system design that either had the rectenna outside the equator area or any satellite not in GEO. The latter is the case for Japanese SBSP concepts as shown in section 1.2.

Despite the lack of engagement by key institutions such as NASA, some U.S. universities still conducted their own demonstrations during this period. For example, the University of Alaska Fairbanks constructed a Semi-Autonomous BEam Rider (SABER) helicopter in 1995 (Hawkins, Houston, Hatfield, & Brown, 1998). It was powered by a 1 kW transmitter operating at 2.45 GHz and showcased at the WPT conference in Japan.

#### *International momentum*

Over the next decades, momentum for MPT increased around the globe. Encouraged by Japan's advances, NASA

performed another comprehensive evaluation of the prospects of SBSP, the positive results of which prompted it to initiate the SSP Scientific Exploratory Research and Technology (SERT) program in 1999. The goal was research on key space solar technologies, including power beaming. As part of this program, a public demonstration was conducted in 2002 at the World Space Congress in Houston by targeting a 5.8 GHz beam at a 1 m rectenna array (Strassner & Chang, 2003a). The system was also equipped with a retrodirective transmitter, allowing the beam to track the receiving aperture while it was moving around the exhibition floor. A RF-to-DC conversion efficiency of 82% was ultimately achieved, once again in line with past results but still lagging behind Brown's record from 1976. At the same congress, Japan exhibited the first fully integrated solar power radio transmitter (Matsumoto, 2002).

Around the turn of the millennium, South Korea also launched its own WPT program through the Korea Electrotechnology Research Institute (KERI), which, based on private communications with external scientists, managed to demonstrate a total power beaming efficiency of 44% with a final DC power output of just over 1 kW (Rodenbeck et al., 2021). If correct, this would be the first result that at least got close again to Brown's 1975 JPL experiment.

While the World Space Congress helped restore momentum to the WPT ambitions of the west, Texas A&M University continued innovating the rectenna with a printed circular polarization design (Strassner & Chang, 2003b). The new approach achieved 78% RF-to-DC efficiency at 5.6 GHz and allowed for 4 times fewer diodes over the surface of the rectenna compared to old designs. Such improvements directly translate into simpler manufacture and overall lower costs, both of which crucial factors for SBSP. At the same time, other American universities tested wideband rectenna arrays to potentially achieve flexibility regarding the transmission frequency but could not achieve significant conversion efficiencies (Hagerty & Popovic, 2001).

Also during this period, while JAXA published its SBSP concepts, Kyoto University developed its Space Power Radio Transmission Systems SPORTS-2.45 and SPORTS-5.8 (Shinohara, Matsumoto, & Hashimoto, 2004). By replacing the standard microwave tubes in the transmitter with phase-controlled magnetrons (PCM), the researchers achieved higher efficiencies at higher kW power levels while also improving beam steering capabilities. This PCM technology was then used in 2008 for a relatively impromptu yet historic joint Japanese-American demonstration in Hawaii (Foust, 2008). Using microwaves, researchers successfully beamed power across the 148 km distance separating Maui from the big island of Hawaii. While beam collection efficiency remained very low at less than a thousandth of a percentage point and power had to be kept low as not to interfere with air traffic, the significance of the demonstration was showing that power could be sent via microwaves across a distance roughly resembling the depth of the earth's atmosphere. Despite the PCMs, keeping the beam on-target proved one of the key challenges. One year later, Kyoto Uni-

versity further tested two 110-W PCMs by beaming power at 2.46 GHz from a blimp to the ground (Shinohara, 2013). The system was also using a pilot signal for beam tracking and reached transmitting antenna efficiencies of 54.6%. It was also around this time that the idea of transparent antenna arrays as discussed in section 2 started taking hold.

#### *Microwave power beaming today*

As momentum continued to build in the last decade, Japan succeeded in multiple large power beaming field experiments as part of its SBSP initiative by the Ministry of Economy, Trade and Industry (METI). Once again displaying the deep involvement of the Japanese private sector, in 2015 Mitsubishi Heavy Industries transmitted 10 kW at 2.45 GHz with an aperture separation of 500 m (Nishioka & Yano, 2015). Thus, they set a new Japanese record for distance and power transmitted. The corresponding efficiency numbers have not been reported. Also in 2015, METI conducted a horizontal power beaming demonstration at the Mitsubishi Electric Facility (Mihara et al., 2015). 1.8 kW were beamed 55 m at 5.8 GHz with a link efficiency of 18.6%. This particular experiment was preceded by lab testing undertaken by J-Space System (Takahashi et al., 2016). The researchers successfully showed that accurate beam targeting could be maintained with the help of a retrodirective subsystem despite temporary misalignments of the antenna panels. As discussed before, such gravitational misalignments would have to be expected for any array-based SBSP system. The most recent Japanese demonstration was held in 2019, where microwave power was successfully beamed at a density of 4 kW/m<sup>2</sup> towards a drone at a distance of 10 m (Shinohara, Hasegawa, Kojima, & Takabayashi, 2019). The 60 W of power delivered, reduced to 42 W at 30 m altitude, successfully prolonged the battery life of the drone.

Today, with a focus on sandwich modules as discussed in section 2, Japan is looking to develop better Schottky diodes to improve efficiencies of the rectification process (Mizojiri et al., 2019). This can be seen as a promising approach, given what Brown was able to achieve with his custom-built diodes. Japan also initially had its first small solar satellite WPT demonstration planned for 2015 (Tanaka, 2021). While it has been delayed due to a lack in technological maturity of WPT systems, amongst other things, Japan still has ambitious goals. A key to their strategy remains the continued development of daily-life use cases together with industry partners for key SBSP technologies such as WPT. JAXA has also communicated plans for more long-distance demonstrations, which will then inform a decision in 2025 on whether to proceed with a demonstration involving a full system in space.

In the meantime, China has also launched multiple WPT research programs at different universities across the country. With its typical ambitious and centrally planned approach, it expects to become the first nation to build a space solar power station with practical value as announced through the China Academy of Space Technology (Lei, 2019). In pursuit of this goal, China has been building a dedicated Space Solar Experiment Base in Chongqing covering 130,000 m<sup>2</sup>, which

will be open to international experts.

Chinese programs have already produced a number of successful demonstrations. In 2014, researchers at Sichuan University beamed a small amount of power via microwaves at 2.45 GHz across 4.5 m, achieving a link efficiency 14.2% (Rodenbeck et al., 2021). Two years later, they experimented with a subarray decomposition of the rectenna at 5.8 GHz, boosting overall efficiency by more than 10% (H. Zhang & Liu, 2016). In 2018, a demonstration in Xi'an also achieved 66.5% RF-to-DC conversion efficiency while using the first focused MPT system with circular polarisation (Dong et al., 2018). During the same year, plans were announced to build an entire SBSP system on the ground for testing, with a targeted beam distance of 100 m, power output of 1 kW, and DC-to-DC efficiency of 20% (Hou & Li, 2021). This project has not been concluded yet. The following year, similar targets were achieved by researchers at Wuhan University at the less commonly used frequency of 10 GHz (Rodenbeck et al., 2021). An approximate link efficiency of 19.5% across 100 m was achieved. The most recent known Chinese demonstration took place at Sichuan University in 2020, with a system operating at 5.8 GHz at 18.5% DC-to-DC efficiency over a distance of 10 m (Chen, 2020). China has also contributed to rectenna designs by improving their heat management, enabling performance at higher power levels (B. Zhang et al., 2015). Overall, China has been able to achieve quite impressive results comparable to other nations, despite having started its efforts rather recently. Nonetheless, the Chinese MR-SPS concept targets a WPT efficiency of 54%, in line with Brown's record. Therefore, demonstrated efficiencies still need to nearly triple to reach that goal.

For the future, China plans to launch tethered balloons with solar panels at its newly built experiment base (Lei, 2019). Once those have reached their operational altitude of 1 km, they will collect energy from the sunlight and beam it down to the ground. There have also been plans for another low-power demonstration at 5.8 GHz across a distance of up to 100 m at the same base (Rodenbeck et al., 2021). However, no updates are available as of yet.

The country of South Korea has also continued its engagement with MPT. A notable advancement are Korean efforts towards better heat management and high-power performance of rectennas in 2018 (Park, Kim, & Youn, 2018), a continuation of previous research by the Chinese. Additionally, in 2019 the U.S. entered into a partnership which resulted in another drone demonstration (Song et al., 2019). 10 GHz of power was beamed at an airship at a NASA facility using 32 rectenna array sheets in total and achieving speeds of 7 mph. In line with this experiment, Korean companies are working on microwave power transmitters in alternative ranges such as the X-band at 7 to 11 GHz (Rodenbeck et al., 2021).

Meanwhile, the U.S. published its D3 Space Solar Proposal in 2016, declaring its intention to become the leader in SBSP (SDSC, 2016) - possibly also in response to Chinese advances. Agencies involved include the Department of State, Department of Defense, DARPA, U.S. AID, NRL, the Air Force, and defence contractor Northrop Grumman. As mentioned in

section 2.3.1, the United States has also conducted its own space tests with the PRAM-FX, during which DC-to-RF efficiencies of 37.1% could be demonstrated (Rodenbeck et al., 2021). These results outperformed previous ground tests of the employed sandwich modules (Jaffe, 2013). The California Institute of Technology is another American organisation deeply involved in research on modular phased arrays, as noted in section 2, including timing devices to achieve synchronization at large scales for focused microwave beams (Gal-Katziri & Hajimiri, 2018).

Recently, another MPT demonstration has taken place in the U.S. to test the practicality of terrestrial microwave power beaming over distances exceeding 1 km (Rodenbeck et al., 2022). As this specific set-up made use of ground bounce properties of microwaves over cluttered terrain to boost power density and efficiency, it is not fully applicable to SBSP use cases. Due to limited aperture sizes and power handling capabilities of the utilized commercially available diodes, which required beam defocusing, overall efficiency was initially limited to 5%. Nonetheless, the ensuing case studies have shown that such a setting could achieve link efficiencies of up to 44%, e.g. by increasing rectenna aperture areas by a factor of 20. This is a relevant result for SBSP, as aperture areas are required and expected to be very large.

Over the next couple of years, the Air Force Research Laboratory (AFRL) will be managing the Space Solar Power Incremental Demonstrations and Research (SSPIDR) project (Rodenbeck et al., 2021). The approach consists of incremental demonstrations and further development of key technologies, including MPT, and is structured in four phases. Ideally, these would then culminate in a fully operational SBSP constellation. The current phase one plans for three major demonstrations. The first, called Arachne, attempts to be the world's first space-to-ground power beaming demonstration by a modular sandwich panel with integrated beam formation optimisation via in-situ array shape measurement and is slated for 2023. The second, SPIRRAL, will test thermal management capabilities of the system and is also planned for 2023. Finally, SPINDLE will test the overall orbital structure deployment. These ambitious projects reflect the opinion of leading American researchers on MPT that the technology has progressed enough to allow for real world developments, as expressed by Rodenbeck et al. (2021).

There are also private companies active in the field of WPT without any direct governmental involvement. For example, Emrod from New Zealand is planning to commercialise MPT (The Economist, 2021a). In collaboration with Powerco, a local electricity distributor, a prototype WPT system has been developed in an enclosed test facility. Next, Emrod plans to beam power in the kW-range from a solar farm to a client some 2 km away. The company claims an efficiency of about 60% and intends to boost this number further by using relays to refocus the beam along the way. This, however, will not be an option for SBSP. Another private sector institution involved is Solaren. The California based company aims to develop commercial SBSP plants to ultimately operate them and sell their electricity (Solaren, 2022). For this purpose,

they are also researching WPT systems but have not published any demonstrations so far.

In conclusion, there have been a number of successful MPT demonstrations over the years, addressing some of the difficulties a system for SBSP at scale might encounter. Great interest in the possibilities of this transmission approach has been evident across countries and driven by a diverse set of actors. However, technical implementation is not the only challenge for power beaming based on microwaves.

### 3.3.2. Spectrum management

One of the bigger challenges for WPT remains spectrum management. Globally, the International Telecommunications Union (ITU) allocates frequencies for different uses (ITU, 2021b). So far, no wavelength in the spectrum has been assigned to microwave power beaming. It would require a long and arduous process through the ITU to achieve that. Additionally, national bodies such as the Bundesnetzagentur (BNetzA) in Germany or the Federal Communications Commission (FCC) and National Telecommunications and Information Administration (NTIA) in the U.S. impose their own rules for spectrum utilisation. This results in a difficult environment for new technologies to gain a foothold and can hamper development and innovation.

Nonetheless, patterns regarding favoured frequencies have emerged over the past decades. As we have seen, most demonstrations take place around the 2.45 GHz and 5.8 GHz frequencies. Both of them reside within the Industrial, Scientific, and Medical (ISM) frequency bands as classified by the ITU (ITU, 2021b). However, this broad definition is resulting in the bands getting crowded. Hence, there was a notable shift in some recent experiments towards higher frequencies around 10 GHz, also known as the X-band. As discussed at the beginning of this section, the atmospheric properties of the X-band are slightly worse yet still comparable to those of lower frequencies.

With this range of possible options, standardisation is key. So far, no regulatory definition of power beaming services exists to clear the path for more focused technological development in harmony with regulatory ambitions. Only Japan is currently making strides to tackle the lack of regulatory support by trying to establish WTP standards through the Wireless Power Transfer consortium for practical applications (WiPoT) and the Broadband Wireless Forum (BWF) (ITU, 2021a).

Potential interference with other services also remains a prominent issue. For example, telecommunication companies in the U.S. do not require licenses to operate in the ISM band. However, they are not allowed to interfere with other devices in the same band, which can limit the effectiveness of power beaming in the ISM. This was the case during the 2008 Hawaii demonstration, where power levels had to be kept subdued, resulting in lower efficiencies. Besides the base frequencies used for WPT, harmonics up to the 10<sup>th</sup> level also need to be filtered to prevent interference with devices operating at these frequencies. This includes other satellites as

well as some of the most restrictive bands reserved for radio astronomy (DoC & NTIA, 2021).

Rodenbeck et al. (2021) have conducted a simulation using the 2.45 GHz (NASA, 1978) and 5.8 GHz SBSP reference systems by NASA (Davis, 2012). As shown in figure 11, side-lobes with significant power levels remain even at high collection efficiencies. As a result, many hundred MW of power would be scattered away from the rectenna, degrading sensitivities of Bluetooth devices or radios for thousands of kilometres away from the rectenna. Harmonics of 2.45 GHz and 5.8 GHz also fall within primary space-to-earth service bands (ITU, 2021b). Consequently, transmitting antennas would have to filter those harmonics down to non-interfering power levels, as existing communication systems are not adapted to deal with these levels of potential interference.

### 3.3.3. Safety

Based on past microwave technologies, safety thresholds for microwave exposure have already been defined by various organisations. In general, the Institute of Electrical and Electronics Engineers (IEEE) considers a power density of about 100 W/m<sup>2</sup> safe for controlled access areas (IEEE Standards Coordinating Committee, 2019). This number does not necessarily constitute a hard physical limit, given that power transmitted by the sun's light can reach 1000 W/m<sup>2</sup> in certain places during the summer (Koblin, Krüger, & Schuh, 1984). However, this increased limit would still be lower than some of the power densities achieved in the past. For example, the 1975 Goldstone demonstration peaked at 1,700 W/m<sup>2</sup> (Dickinson, 1975).

Hence, systems must be in place to ensure that adequate limits are not exceeded and that the beam remains on target. The necessary steps are often referred to as the "6 Ds" (Rodenbeck et al., 2021). In particular, they specify that a system should be able to Detect any potentially unsafe situation in order to then Decide whether to Defocus, Divert, Dim, or Douse the beam. Nonetheless, most demonstrations have stayed well within these limits and diffraction physics also mean that over the large distances SBSP requires, power will inevitably spread out. The latter would be conducive to lower power densities as measured in W/m<sup>2</sup>, suggesting the clear possibility of a safe MPT environment. Once again, uniform standards appear key to develop the technology towards a safe direction.

### 3.4. Laser power beaming

Microwaves are without question the modality of choice for all major power beaming concepts. Nonetheless, laser power beaming made some recent progress and is hence included in this analysis as a somewhat possible alternative. A chief benefit of LPT is without a doubt the smaller scale of the systems involved. Given the much smaller wavelength when compared to microwaves, the sizes of transmit and receiver apertures are a fraction of those of MPT systems. For instance, an optical beam near the infrared spectrum at 795 nm would require a receiver of only a few meters in diameter

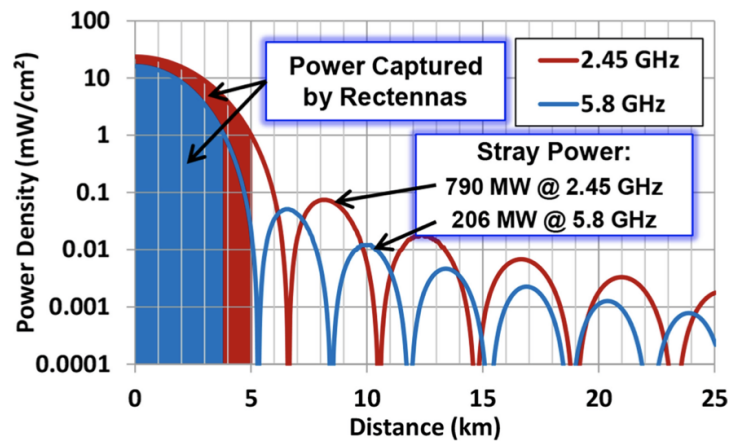


**Figure 11:** Sidelobe patterns for the 2.45 and 5.8 GHz NASA SBSP reference systems. (Rodenbeck et al., 2021)

(Rubenchik, Parker, Beach, & Yamamoto, 2009) as opposed to the kilometer-scale rectennas used for microwaves. These considerations were first introduced into the discussion in the early 2000s (Penn, Law, et al., 2001).

Additionally, laser beaming from space could make use of so-called direct solar pumped lasers, which use concentrated solar irradiation directly as an energy source for the beam formation in the gain medium without the need of going through an electrical conversion first (Summerer & Purcell, 2009). This bears the potential of lower conversion losses and the avoidance of high voltages on the space segment. However, they prove difficult to scale to SBSP levels and heat management of the laser generating segment remains an issue.

On the receiver end, PV cells specifically designed for the transmission wavelength of the laser could be used. Therefore, these cells can be fine-tuned for a small portion of the spectrum instead of for the majority of it like standard PV cells (York & Fafard, 2017). Such specialized multijunction cells are pushing monochromatic optical-to-DC conversion efficiencies close to 70 %, approaching those of rectennas.

Due to the long distances across which power must be transferred for SBSP, fibre lasers promise to be a well-suited variant based on their high levels of brightness and beam quality (Grandier et al., 2021). Overall, they are characterised by superior heat management when compared to conventional lasers, high efficiencies due to the use of laser diodes, and good scalability of optical power. As a result, conventional fibre devices can achieve link efficiencies in the range of 20% to 30%.

Finally, beam tracking is also of great importance to LPT systems, particularly because the target is much smaller. The same retrodirective approaches introduced for microwave beams and involving a pilot signal could also be applied to lasers (Summerer & Purcell, 2009). The concept of array building to overcome hardware scalability issues is likewise a theoretically viable alternative for lasers.

#### 3.4.1. Selected demonstrations

So far, there have been a number of notable laser power transmission demonstrations, particularly in recent years. In 2004, Japanese scientists developed a set-up intended to use a laser to beam power to a rover looking for ice on the moon (Kawashima & Takeda, 2004). In a terrestrial demonstration with a life-size rover, power was beamed across a distance of 1.2 km with a link efficiency of more than 20%.

Laser transmission was also investigated in the context of powering robots or aerial vehicles. One such demonstration using a 200-W laser at 808 nm achieved output power levels of 40 W at the target, resulting in a link efficiency of 20% (Kawashima & Takeda, 2008). However, the large amounts of dissipated heat when output power was increased above a couple hundred watts and the lack of compact cooling systems suitable for such high-power lasers remained an issue.

More recently in 2014, a high-power transmission system was demonstrated by Chinese researchers for a distance of 100 m and employing a 793-nm wavelength (Tao et al., 2014). Using multijunction GaAs cells for reconversion, the optical-to-DC conversion efficiency remained subdued at 40 %, resulting in a link efficiency of 11.6%. Nonetheless, a power density of 60,000 W/m<sup>2</sup> was measured. Such high levels are indicative of why safety is of an even higher importance for laser-based transmission systems. We briefly explain some safety thresholds and mechanisms in the following section.

Japan has also conducted a laser power transmission demonstration in 2016, in which a beam was sent from the top of a tower to a receiving station on the ground, thereby bridging a vertical distance of 200 m (Tanaka, 2021). At 1070 nm and an output power of 350 W, 74.7 W were ultimately received on the ground. This results in a link efficiency of about 21%.

The most recent and most advanced demonstration took place in 2019 at the U.S. Naval Surface Warfare Center in Maryland (NRL, 2019). In collaboration with the private company PowerLight Technologies, the NRL conducted the

Power TRansmitted Over Laser (PTROL) project. It consisted of a 2-kW laser transmitter and a receiver specifically optimised for the laser's wavelength. Ultimately, 400 W were beamed across a distance of 325 m and converted back to AC to power lights, several laptops, and a coffeemaker. A key challenge during the project included interference with the weather, such as snow or rain. Unfortunately, the achieved link efficiencies were not openly communicated.

### 3.4.2. Safety

Similar to microwaves, there are organisations which have defined exposure limits for optical beams. For instance, the Laser Institute of America (LIA) publishes a series of safety guidelines and standards through the American National Standards Institute (ANSI). Recent standards put the limit at 1,000 W/m<sup>2</sup> (The Laser Institute, 2014). However, as was demonstrated during the Chinese experiments, these limits can be exceeded. Especially in the military, the threshold is commonly crossed if other safeguards are in place that make it highly unlikely for anyone or anything to be exposed to the beam directly.

One innovative approach for such a safeguard system was also on display during the 2019 demonstration by the NRL. By employing guarding sensors which figuratively caged the beam, objects could be detected before they reached it and the system would be turned off (Nugent, Bashford, Bashford, Sayles, & Hay, 2020). It could then restart automatically in a few seconds after confirming that there were no longer any foreign objects in the beam's path.

### 3.5. Conclusion

Across the different power beaming modalities, microwaves seem to have been established as the technology of choice. While lasers offer the possibility of smaller aperture sizes and hence decreased space segment mass, their poor weather penetration characteristics and lack of cost-efficient scaling pose significant hurdles to their implementation in SBSP systems. Consequently, all major advanced concepts so far rely on MPT.

For microwave-based approaches, there have been many successful demonstrations over the past decades. These prove the technical practicality of the technology. Still, none of the distances so far have come close to what would be required of a space-to-earth WPT. Consequently, the scale of transmitting and receiving apertures has also remained limited compared to the km-size structures necessary for SBSP. A comparison of orbital distances for different concepts and the maximum achieved can be found in table 3.

Many of the records for beaming efficiencies established by Brown in the 70s and 80s still stand to this day. Specialized hardware tailored to MPT instead of general RADAR applications has played an important role in his achievements and will be required again to maintain the efficiency levels necessary for SBSP. However, the overview in table 3 also shows that the conversion efficiencies achieved during demonstrations are already in line with what major SBSP concepts

expect. The persistent misconceptions about its feasibility therefore seem unfounded and based on misconceptions regarding the technology and associated far-field assumptions (Shinohara, 2014).

The contribution of the WPT segment towards LCOE also mostly comes from the amount of energy that is transmitted and the cost of the rectenna. Variance analyses for LCOE so far suggest that the latter does not have a significant impact relative to the other cost positions (e.g. Way & Lamymann, 2021a). Therefore, a trade-off between an increased aperture size to maximise microwave collection efficiency and increased construction costs might be beneficial.

Overall, as space is getting more commercial and political, momentum for WPT in a space setting is increasing. Another indication for this dynamic is the most recent wave of in-space demonstrations and China as a notable new entrant into the field. Especially the U.S. will see itself pressured not to be left behind by ambitious Chinese WPT targets. Nonetheless, it is critical for the main actors to define a common regulatory definition of the technology around which standards could be formulated. Such shared frameworks would help overcome the remaining challenges regarding spectrum and safety management and include starting or supporting the necessary processes within the ITU. Furthermore, early engagement with society at large to educate them on WPT could help drive the social acceptance of the technology.

## 4. Infrastructure and manufacturing

Having covered the space segment as well as the energy transfer to earth, we now take a look at the production and infrastructure necessary for SBSP. During our brief analysis of the manufacturing side, a particular focus will be placed on economies of scale and first considerations regarding the life cycle of the system. For the required infrastructure, ongoing developments in the launch market play a critical role in determining the technical and economic feasibility of SBSP. As part of this, we will also discuss some of the orbital considerations and implications of the chosen orbit on capacity and cost. Overall, launch infrastructure and capacity will be the focus of this chapter.

### 4.1. Metrics for infrastructure and manufacturing evaluation

For the production, launch, and orbit of SBSP systems, the following metrics were determined to be of importance to gauging overall system performance.

#### *Mass-specific costs [\$/kg]:*

This metric measures the costs incurred per unit mass of the SBSP system to render it operational and can relate to a number of processes. First, the average production costs of the sandwich modules and other components for the satellite as well as the rectenna can be measured in a comparable way

**Table 3:** Comparison between the MPT metrics targeted by major SBSP concepts and what has been achieved during power beaming demonstrations. While no distances in the same order of magnitude have been achieved, transmission efficiencies are already at or above the desired levels.

	Beaming modality	Frequency [GHz]	Efficiencies			Distance [km]	Power density [W/m <sup>2</sup> ]	
			DC-to-RF	Collection*	RF-to-DC			Link
<b>Concept target metrics</b>								
SPS-ALPHA	Microwave	2.45	70.6%	83.3%		58.8%	36,000	85
CASSIOPeiA	Microwave	2.45	85.0%	82.0%	85.0%	59.2%	36,000	60
MR-SPS	Microwave	5.80	83.3%	90.0%	76.5%	57.4%	36,000	73
<b>Demonstrated values</b>								
Maximum achieved	Microwave	2.45 - 10.00 <sup>†</sup>	>70.0%	>90.0%	91.4%	54.2%	148	1,700

\* Based on diffraction physics, mostly depends on relative antenna/rectenna dimensions, distance, and beam steering capabilities

† Range of all performed demonstrations

using mass-specific costs. Second and arguably more importantly, launch costs are measured in dollars per kilogram payload. Overall, this metric can then be used to put a dollar value on some of the calculations from section 2.

#### Launch capacity [t/a]:

The launch capacity per year denotes the total mass that is transferred into space throughout a certain time period, for instance a year. Due to the long lead times in the launch market, this number can either be based on past realised launches or services already locked in for the near future. Given the great mass of all SBSP satellite concepts, launch capacity is critical in determining the time scales over which a space vehicle could be established in orbit. It should further be noted that far from all of this capacity would be available to SBSP, as other projects have already booked their launches and some lift vehicles might be incompatible with SBSP components.

#### Energy payback time [days]/[months]:

Energy payback time measures the period it would take, often in days or months, for a given SBSP concept to earn back the same amount of energy that was used to render it operational. This includes energy embedded in materials and expended during production processes as well as the energy necessary to transport all components into orbit. The metric enables us to analyse how long it takes to amortize the energy invested into SBSP generation capacity.

#### Emissions factor [g CO<sub>2eq</sub>/kWh]:

Given that SBSP is intended as a renewable energy source, it is important to determine the amount of emissions associated with its energy production and resulting from all stages of its life cycle, including those by some of the required infrastructure, such as launch systems. While we focus on greenhouse gas emissions, the impact can also be extended to all kinds of externalities. For instance, the use of critical raw materials or land use of the rectenna are outside the scope of this thesis but also important when considering the sustainability of SBSP systems.

Based on these four metrics, we now evaluate some of the production and infrastructure necessary to facilitate the large-scale employment of SBSP. We begin with a closer look at manufacturing, assembly, and maintenance dynamics followed by an analysis of the space launch market.

#### 4.2. Manufacturing, assembly, and maintenance

So far, many satellite manufacturing projects have been marred by long delays and large cost overruns. One recent example of this is the James Webb Telescope. Initial cost targets were in the range of \$ 1 billion to \$ 3.5 billion with the launch slated for 2011 at the latest (Greenfieldboyce, 2021). Ultimately, the space telescope cost more than \$ 10 billion dollars and was only launched in 2021. One of the factors driving this disadvantageous dynamic is the lack of economies of scale. Large projects such as the Webb Telescope are complicated one-off satellites with little modularization.

However, scientific satellites' primary goals are not of an economic nature. Conversely, SBSP heavily relies on economies of scale to bring production costs down and accelerate manufacturing processes to ultimately achieve economic competitiveness. Here, modularizing the satellite and rectenna design as much as possible is an important enabler and hence pursued by most concepts as discussed in section 2. Generally, modularity is the idea of dividing a system into smaller elements that can be designed, optimized, and manufactured independently around common measurements and consequently exchanged with other modules in the future (O'Quinn & Jones, 2022).

Recent years have also seen a drastic increase in the amount of commercial satellite projects, which helps fuel cost optimization in space manufacturing through learning curves. Learning curves represent a decrease in specific costs as devices are produced repeatedly and hence the process can be optimized. Typically, the learning factor in the aerospace sector amounts to about 85% (Madonna, 2018). This means that each new batch benefits from a cost reduction of about 15%, reaching a limit once around 50% of initial costs are

reached. The learning factor of 80% assumed for the SPS-ALPHA concept is therefore roughly in line with the industry (Mankins, 2017).

One recent example of strong learning curves as a result of mass-manufacturing modular space vehicles is the solar-powered Starlink system by SpaceX. The company has communicated a per satellite cost for its 4,400-strong initial LEO constellation of well below \$ 500,000 at a weight of 275 kg (Mankins, 2021). Calculating an upper bound for specific cost, this results in about 1,800 \$/kg, only a fraction of the roughly 300,000 \$/kg for standard early satellite types. Most concepts plan to bring hardware costs even lower, with SPS-ALPHA aiming for less than 1,000 \$/kg. Regarding manufacturing speed, SpaceX manages to produce about 120 satellites or 33 t per month. This compares to a weight of 2,000 t and a planned construction time, including in-space assembly, for even the lightest SBSP concept of only two years (Way & Lamyman, 2021a).

The difficulty with such modular mass-manufacturing is that it still needs to adhere to high quality and precision standards. Particularly with the RF transmit and receiver elements, uniformity directly translates into system efficiency. For instance, rectenna panels need to show equal DC outputs across all elements to maximise efficiency (Shinohara & Matsumoto, 1998). Furthermore, there is a trade-off between additive manufacturing techniques that could be employed to produce flexible integrated PV and RF sandwich sheets and modular approaches where PV and RF surfaces can still be separated for easier maintenance (Borgue, Panarotto, & Isaksson, 2019).

Related to this, modularisation also proposes great benefits during assembly, scaling up of pilot systems, and maintenance. Given the reliance by all selected concepts on autonomous robotic in-space assembly, having large numbers of identical parts makes this task much easier and allows modules to be added or replaced with relative ease within the overall system constraints. For this purpose, SPS-ALPHA is planning to utilise hexagonal shapes as a common geometry among most of its components (Mankins, 2021). This includes frames, tiles, reflectors and trusses.

Nonetheless, the robots required for such an assembly are arguably also one of the least developed technologies related to SBSP. Given the relevance of such capabilities across the entire space sector, the European Commission has sponsored the MODular Spacecraft Assembly and Reconfiguration (MOSAR) project to support the development of an autonomous in-space assembly system. After first designs for walking robots have been developed where the two extremities act as legs and arms in an alternating fashion, testing under space conditions is now ongoing (Letier et al., 2019).

Regarding the environmental impact, current assessments show that about 85% of the life cycle impact of a satellite comes from the production of the spacecraft, the launcher, and propellants (Wilson, 2019). Consequently, the technologies and components employed should also be selected for their total impact, including environmental aspects. For instance, there is a large spread in related emis-

sions for different PV technologies discussed in section 2.2. While relatively standard silicone cells tend to have some of the highest resulting emissions, the metrics for newer technologies can vary strongly (Ludin et al., 2018). Perovskite cells, which we have established as a desirable technology option in chapter 2, can result in anything from 50 to 500 g CO<sub>2eq</sub>/kWh. This reflects their comparatively low technological maturity and unstable operational lifetime. On the other hand, quantum dot cells display very low emissions at up to 5 g CO<sub>2eq</sub>/kWh. In concert with other technologies such as nanowires, quantum dots also offer the possibility of reducing embedded emissions further by eliminating the cover glass. Overall, system emissions for SBSP have been estimated to go as low as 20 g CO<sub>2eq</sub>/kWh (URSI, 2007).

For the end of life, most concepts plan to transfer the satellite into a graveyard orbit as deconstruction would be prohibitively expensive (e.g. Way & Lamyman, 2021a). The exact impacts of moving such a large structure to a graveyard orbit where many other decommissioned satellites can also be found has yet to be determined. Potential collisions could aggravate any of the debris-related issues already present today and create problems for other satellites that are still in service as well as future launches.

Regarding energy payback times, studies in the early 2000s have suggested that these are very competitive compared to terrestrial solar and wind. If only 0.5 GW of SBSP were to be installed, the energy breakeven point including manufacturing would be reached after two years (Summerer & Ongaro, 2005). As the capacity of the system is increased, this quickly falls to below six months, about half as much as other terrestrial renewable technologies. The energy required for transporting the components into orbit plays a significant role in these calculations and is therefore further discussed in the following section.

#### 4.3. Space launch infrastructure

The launch of the components for the space vehicle constitutes a critical step and simultaneously a potential bottleneck for SBSP development. Space launches and the deployment of any asset into orbit have always been a complex and until recently very costly endeavour. Historically, only some of the world's most ambitious and wealthy countries had access to space through government-funded projects. However, over the last decade, closer involvement of the private sector has upended the launch market and fundamentally shifted these dynamics. Today, there is a multitude of commercial players around the globe which are offering or currently developing launch services for different applications. We begin by analysing these changes from a cost and capacity perspective and follow up by some environmental and energy considerations.

##### 4.3.1. Developments in the launch market

The advent of reusable rocket boosters fuelled by NASA's approach to sponsor commercial competition in the launch market has led to a steep decrease in specific launch costs

(Jones, 2018). In figure 12, we have visualised these dynamics by launch vehicle weight class. While no universal definition for these buckets exist, light-lift vehicles correspond to a maximum payload of 2,000 kg to LEO, medium-lift reaches up to 20,000 kg capacity, and heavy-lift vehicles are anything above that (Roberts, 2020). Specific launch costs are then calculated using the mission cost, including all direct and indirect positions, and the maximum payload mass, assuming the rocket is fully expendable and not reused. A configuration for reuse limits the payload mass as additional fuel has to be loaded for the booster to navigate back to earth. Furthermore, it should be noted that for satellites that have their own propulsion system, their mass does not equal launch mass as in-space propellant has to be added.

Looking at the specific launch costs to LEO in figure 12, we can see that the decline is particularly pronounced with medium- and heavy-lift vehicles. One factor in this dynamic is SpaceX. Its Falcon 9 rocket at 2,600 \$/kg and Falcon Heavy at 1,500 \$/kg are far ahead in terms of price competitiveness compared to any of the other vehicles in operation.

However, launching to geostationary transfer orbit (GTO) instead of LEO as would be required for SBSP changes the equation to some degree. GTO is a transitory orbit that allows the payload to attain GEO with the help of its own on-board propulsion. Consequently, the price per kilogram payload increases. The extent of this change can be shown with some examples. The mission cost for SpaceX's Falcon 9 lies at \$62M (SpaceX, 2022). If GTO is targeted instead of LEO, payload capacity decreases by a factor of nearly three from 22,800 kg to 8,300 kg. As this assumes a fully expendable rocket, a mission centred around reuse will bring that number down to 5,500 kg. This would result in specific launch costs of 7,500 \$/kg and 11,300 \$/kg, respectively. The price increase is even more pronounced with the Falcon Heavy. At \$97mio per launch, capacity roughly halves from LEO to GTO to 26,700 kg and mass-specific cost more than doubles to 3,600 \$/kg. As the Falcon Heavy configuration includes multiple boosters, having all of them return to earth after depositing the payload lowers these values significantly to a capacity of 8,000 kg at 12,100 \$/kg.

In conclusion, GTO commands a price premium by a factor of about two to three above standard launches to LEO, even without reuse. Only looking at launch costs to LEO can therefore be misleading when evaluating the cost performance of SBSP launch infrastructure. Nonetheless, the cost to GTO employing an expendable Falcon Heavy would be below the expectation of 5,000 \$/kg by some concepts, such as CASSIOPEIA (Cash, 2019).

For the near future, a variety of actors are developing new launch systems which are expected to bring GTO costs down even further. Jeff Bezos' company Blue Origin is looking to transport up to 13,000 kg to GTO (Blue Origin, 2022). To achieve the 5,000 \$/kg level, mission costs would have to stay below \$70M, which is a reasonable level compared to other vehicles. A joint venture by the defence contractors and aerospace companies Boeing and Lockheed Martin called the United Launch Alliance is also planning to fly its Vulcan

rocket for the first time next year (Clark, 2015). The cost target of \$100M per mission and a capacity of 13,000 kg to GTO would result in specific costs of about 7,600\$/kg.

In comparison, SpaceX's Starship, which has already undergone first flight tests, could drastically undershoot these price levels. Aiming for mission costs of \$10M (Roulette, 2022), a 21,000-kg capacity to GTO would result in only about 500 \$/kg, a significant decrease from current levels (SpaceX, 2020). Should additional propellant for the launch system be parked in orbit in advance to decrease the amount required on board during launch, an additional decline by a factor of five would be possible as payload capacity to GTO increases to 100 t. NASA also has its Space Launch System in the pipeline, but further specifications have yet to be communicated.

All these new systems would greatly increase the overall capacity of the launch market. Over the last decade, 2,604 t of satellites have been launched into orbit (Euroconsult, 2021). For the next decade, this number is expected to more than double. Nonetheless, more than 550 t per year of total mass launched would compare poorly to what is required to make an entire SBSP system operational. Even if all this capacity were to be used only for the 2,000-t heavy CASSIOPEIA system, it would take four years just to transfer all components into space. For the heaviest concept, MR-SPS, this number would rise to 20. Therefore, launch capacity for now appears to be a serious bottleneck outside the economic considerations for the system.

Furthermore, the lack of common launch or payload interfaces between rockets complicates stowage and load planning, even if all launch systems were available (O'Quinn & Jones, 2022). Despite adaptations towards the commercialisation of satellites, the launch process remains fairly inflexible with periods from booking to actual lift-off reaching two years or more and exact mass properties being required up to 8 months in advance (SpaceX, 2021). With such long lead times and none of the concepts even in the process of manufacturing a prototype yet, the risk remains that launch capacity will be tied up by other projects for the foreseeable future.

In order to utilize the increased payload capacity of launches to LEO and to minimize the need for in-space propellant on board the satellite when transferring to GEO, William Brown has also come up with a concept called Transportronics (Brown, 1992). In essence, the concept would make use of a narrow microwave beam on earth powered by terrestrial renewable energy to fuel a transport device. This transport device would then be able to move satellites from LEO to GEO at low cost, coupled with unprecedented speed for an electronic launch system, and eliminate the need for more costly direct launches to GTO. In the initial study, a system scale up to transfer up to 60,000 t per year was considered as feasible. However, little has come of the idea since.

With the increase of commercial activity in space, a general trend towards smaller and cube satellites has also been observable (O'Quinn & Jones, 2022). This is further reflected

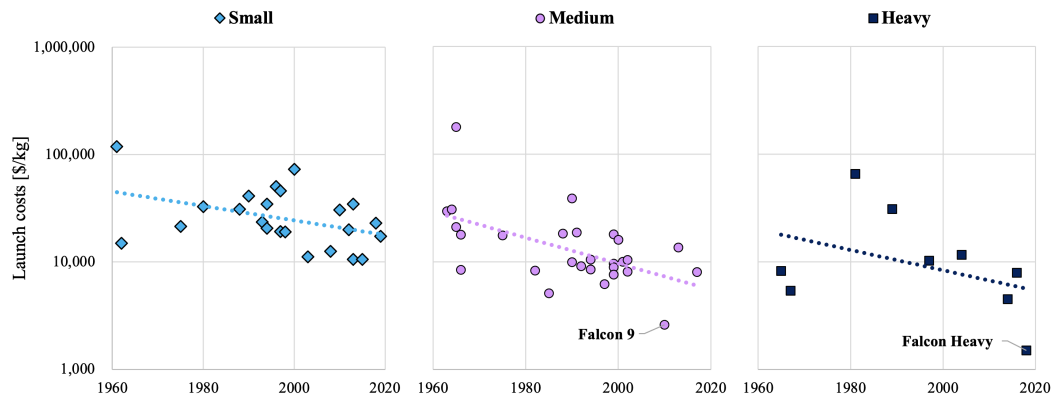


**Figure 12:** Development of mass-specific launch costs to LEO for different launch vehicle classes with trend lines, measured in 2021 dollars. Own analysis based on data from the Center for Strategic and International Studies (Roberts, 2020)

by the fact that while launched mass is set to double over the next decade, the actual number of satellites put into orbit will more than quadruple (Euroconsult, 2021). As a result, many launch providers are also specializing in smaller satellites, contrary to what a SBSP space vehicle would require. Therefore, modularity is also critical to make SBSP compatible with as many launch systems as possible.

#### 4.3.2. Environmental and energy payback considerations

The environmental impact of rocket launches strongly correlates with the type of fuel that is used. In the past, solid fuels were the dominant variant (Dallas, Raval, Gaitan, Saydam, & Dempster, 2020). However, due to their ozone-depleting and toxic characteristics, which were particularly observable in Kazakhstan as the former base for Soviet launches, the launch market is moving to alternatives. Looking forward, liquid hydrogen (LH2) and oxygen (LOx) as well as kerosene are likely to become more dominant. While LOx/LH2 fuels are difficult to handle due to the temperatures required, they provide great energy output and only result in water vapour when burnt.

Nonetheless, the entire SBSP system and the launch infrastructure in particular will require a full life cycle analysis (LCA). First analyses based on a framework developed for space missions by Wilson (2019) show that the most significant environmental impacts of space launches include climate impacts, toxicity, acidification, and debris. In particular, the potential to cause ozone depletion, freshwater aquatic ecotoxicity, and air acidification are the prominent three effects. Based on the numbers compiled by Wilson (2019) for 2018, the emissions impact of a single space mission is more than 1,000 times greater than that of the average global flight. Given the expected expansion in the sector, close attention will therefore have to be paid to these environmental effects and options that minimise negative externalities. For instance, LOx/LH2 fuels where the hydrogen is generated via green electricity promise to be one of those sustainable alternatives.

The fact that hydrogen can be produced via electrolyses also offers the potential for SBSP to recoup the fuel that was

used to put the system into space directly. It roughly takes 32 kWh in propellant to move one kilogram from the earth's surface to GEO (Mankins, 2017). Based on that metric, it would take CASSIOpeiA just over one day, SPS-ALPHA five days, and MR-SPS one and a half weeks to generate the same amount of energy that was used in the form of fuel. If the systems were to produce their own LH2-based propellant, for instance during times where terrestrial solar and wind on their own are sufficient, we would also have to account for the energy lost during conversion steps and required for liquefaction. Consequently, the payback time would increase to about three weeks for CASSIOpeiA, three months for SPS-ALPHA, and half a year for the comparatively heavy MR-SPS. A summary of these energy payback times is also provided in table 4.

#### 4.4. Conclusion

Overall, a modular approach to any SBSP concept will be critical to enable economies of scale during manufacturing, compatibility with as many launch systems as possible given the recent trend towards smaller satellites, and ease of assembly as well as maintenance. The Starlink project has successfully shown that manufacturing at comparatively low mass-specific cost is possible already. While the amount of Starlink modules only number in the low thousands, SBSP concepts would far surpass that amount, potentially unlocking greater learning curves.

The continuous decline in launch costs driven by the commercialisation of the launch market also promises to further enhance the economics of SBSP. Based on some of the variance analysis for LCOE in the literature (e.g. Way & Lamyman, 2021a), launch costs are even a particularly strong lever. However, our analysis suggests that total payload capacity will lag behind what would likely be required to transfer an entire SBSP system to space for the foreseeable future. Upcoming heavy-lift vehicles such as Vulcan, Starship, and SLS might be able to alleviate this bottleneck to some degree. Nonetheless, their exact market entry is as of yet unknown. Additionally, the long lead times in the market could make it difficult to achieve any meaningful presence in orbit over

**Table 4:** The amount of time it would take for different SBSP concepts to feed the amount of energy required to put them into space back into the grid. The first number is a simplified comparison, only considering the energy content of the fuel used for a launch to GEO. The second number also accounts for all conversion steps necessary to produce green LH2, using the electricity generated by SBSP. Own analysis based on data from [Cash \(2021a\)](#) and [Mankins \(2017\)](#).

	Energy payback time [days]	
	Energy content of fuel needed for launch to GEO	Energy needed to produce green LH2 propellant for launch to GEO
Concepts		
SPS-ALPHA	5.0	91.7
CASSIOPeiA	1.3	23.0
MR-SPS	13.3	242.4

the next couple of years. Therefore, the commonly in the literature observable singular focus on launch costs might be misguided as the true constraint potentially lies in the availability of payload space.

Environmentally and from an energy perspective, the literature suggests that SBSP at scale has shorter energy payback times than conventional renewables at relatively low emissions. Furthermore, a shift towards more sustainable rocket fuels could help lower emissions by using green energy to produce the liquid hydrogen utilized by the launch vehicles. Nonetheless, given the majority of impacts arise during the manufacturing process of the mission, particular focus will have to be placed on using sustainable materials and processes. So far, it seems that some of the technologies introduced in section 2.2 such as quantum dots could meet this requirement. At the end, a holistic LCA will be necessary to fully understand all the impacts of SBSP. Particularly [Wilson \(2019\)](#) has developed a framework that could be applicable to such an analysis of SBSP.

## 5. Summary and outlook

SBSP combines two of the most dynamic industries of our time: renewable energy and space. It is unique in its potential ability to offer flexible renewable baseload power that is dispatchable on a semi-global scale. Such capabilities would constitute a crucial step in securing energy security for the electrification of our economy. There are already a number of concepts that have been far advanced in their planning stages, often with direct government involvement and support. Nonetheless, none of them have produced a full-system prototype yet.

For our analysis, we have divided the general SBSP model into three segments: the space segment, wireless power transmission (WPT) and ground structures, and manufacturing and infrastructure. Based on the metrics defined for each of those, we have seen that some factors remain which are still holding SBSP back from becoming a reality. When it comes to solving these issues, we are often faced with trade-offs between different system parameters. The right solution will ultimately have to be found through prototyping and demonstrations, which should be the priority for any SBSP design going forward.

One of the biggest levers to improve the economics of the space segment are weight and power. Hence, mass-specific power and aerial density were identified as crucial determinants of space segment performance. Out of the three investigated concepts, CASSIOPeiA achieved the highest mass-specific power by a notable margin at 1.51 W/g. These results indicate that the consequent use of sandwich modules and boosting of PV power through solar concentration are essential in achieving competitive performance levels. This was particularly evident with the Chinese MR-SPS concept, where the lack of PV and RF surface integration as well as non-existent solar concentration led to some of the poorest results at 0.16 W/g. However, SPS-ALPHA also shows that sandwich modules as well as any reflector arrays and structures have to be lightweight so their benefits are not neutralised by the additional mass.

Still, even for CASSIOPeiA there appears to be room for improvement. We have been able to identify a number of technology alternatives that promise to reduce weight, improve power levels, and enhance inherent radiation resistance. Some approaches could even deliver multiple of these benefits at once. For instance, LSCs bear the potential to increase PV cell performance while maintaining a flat-plate tile geometry and even boosting radiation resistance. Nanowires could complement any design to drastically reduce radiation damage and increase the useful lifespan of the space segment while eliminating the cover glass. Making such protective but weighty components redundant could boost mass-specific power by a factor of nearly three. Lastly, pervoskite as a cell material has the potential for significant synergies with the aforementioned technologies, based on its self-healing properties and exceptionally high power output. However, uncertainties regarding the efficiency levels of all three of these alternatives, particularly when under high thermal stress, will have to be addressed before they can be fully implemented. Nonetheless, even based on their current performance levels they appear competitive, suggesting that foregoing some efficiency to significantly reduce mass might be an approach worth pursuing.

On the other hand, not all investigated options appear to work for SBSP systems. Despite having by far the highest mass-specific power at more than 2 W/g, integrated

parabolic mirrors appear to be an infeasible solution as they are difficult to mass-manufacture and notably constrain satellite architecture. But even with the flat-plate module design maintained, the challenge of achieving a continuous duty cycle remains. Our two proposed solutions of dual-sided sandwich modules for planar arrays or L-shaped modules for helical arrays both come with inherent trade-offs. While the former results in an increase in complexity, weight, and hence cost, the latter requires heavy reflector structures and has limited scalability. Ultimately, both designs might be viable within the right setting. However, planar arrays would still require extensive attitude control and adjustment maneuvers, even when employing dual-sided tiles.

For the transmission segment of the system, efficiencies are a key determinant of subsystem performance as they dictate the amount of energy that can ultimately be fed into the grid. Given the need for atmospheric and weather penetration as well as scalability, microwaves appear to be the modality of choice, beating out lasers, who particularly struggle when it comes to those two characteristics. We have shown that there is an extensive history of successful MPT demonstrations, achieving and even surpassing the link efficiencies of above 50% targeted by today's most advanced concepts, such as CASSIOPEIA or SPS-ALPHA. The prevailing notion based on far-field assumptions that MPT cannot achieve the performance levels necessary for SBSP therefore appears to be unfounded.

Nonetheless, the distances across which power has been beamed and the corresponding scale of transmit and receiver apertures still lags behind what would be required for a space-to-earth system. This raises the questions of whether the success of terrestrial demonstrations will ultimately be transferable to the space environment. Ongoing and upcoming WPT experiments should help in overcoming these uncertainties, as the technology enjoys considerable momentum due to its applicability outside of SBSP.

The biggest remaining complication appears to be the question of spectrum management. With no regulatory definition of WPT and hence no internationally allocated bandwidths, there is no common frequency around which systems could be optimised and advanced. As a result, each actor is left to define their own standards. Japan, a notable contributor when it comes to starting the necessary processes at the ITU, should therefore be supported in its efforts by other countries to the benefit of everyone pursuing this technology.

Lastly, we analysed the manufacture and infrastructure subsystem with a particular focus on the launch market. For the construction of the satellite and ground structure, economies of scale through modularisation appear crucial to unlock cost benefits. The example of Starlink has shown how far-reaching these advantages can be. Nonetheless, while a first analysis suggests energy payback times and environmental impacts from the manufacturing process are manageable, in-depth environmental studies and LCAs are required to ensure the overall sustainability of the technology. Furthermore, many approaches to SBSP rely on autonomous robotic assembly and maintenance once in space. However, this

technology is as of yet untested in a practical setting, despite being so crucial to the success of these concepts.

When examining the transfer from earth to orbit, launch costs are often cited in the literature as a primary concern and obstacle for the realisation of an economically viable SBSP system. Fortunately, the commercialisation of the launch market over the last decade has brought prices down by orders of magnitude while capacities are still expanding, enhancing SBSP economics in turn. Furthermore, greener fuel alternatives such as propellants based on LOx/LH2 offer the possibility of significantly reducing some of the environmental issues that have raised concerns about rocket launches in the past.

Nonetheless, it appears questionable whether the 550 t of planned total yearly launch capacity over the next decade will be enough. Given that most of that capacity would not be available on an exclusive basis, even the lightest concept CASSIOPEIA could arguably not be transferred into orbit within a reasonable timeframe. Additionally, the long lead times for launch missions plus a lack of common payload interfaces make it very difficult to flexibly spread out space transfer operations across multiple different lift vehicles. The recent trend towards smaller satellites, which is also reflected in the reduced payload capacities of many upcoming new launch systems, further underlines the need for a modular approach to ensure compatibility with these small-scale lift vehicles. Consequently, our analysis suggests that launch capacity rather than cost might be the determining aspect concerning the operationality of SBSP. A reduction in mass would then not only be a matter of economics but might be the factor that would render such a project possible in the first place.

In conclusion, we were able to identify a number of technology alternatives that have the potential of improving critical subsystem metrics to ultimately enhance SBSP system economics. These could lead to SBSP being an overall competitive renewable energy alternative to drive wide-spread electrification of industries. The exact magnitude of these economic benefits will have to be confirmed through dedicated LCOE studies. Furthermore, our analysis based on past demonstrations suggests that WPT is already at a stage where, if scaled up, could deliver the required transmission capabilities. However, the launch infrastructure appears to be the critical bottleneck that could prevent any SBSP system from advancing past the planning stage in the foreseeable future. If these capacity constraints are not addressed, the future of SBSP will likely remain uncertain.

## References

- Abdelal, G. F., Gad, A. H., & Abulfoutouh, N. (2013). *Finite element analysis for satellite structures - applications to their design, manufacture and testing*. Springer.
- Akiba, R., Miura, K., Hinada, M., Matsumoto, H., & Kaya, N. (1993). ISY-METS rocket experiment. *The Institute of Space and Astronautical Science report*, 652, 1–13.
- Andreev, V. M. (2018). GaAs and high-efficiency space cells. In *Mcevoy's handbook of photovoltaics* (pp. 421–438). Elsevier.
- Barrigón, E., Heurlin, M., Bi, Z., Monemar, B., & Samuelson, L. (2019). Synthesis and applications of III–V nanowires. *Chemical reviews*, 119(15), 9170–9220.
- Blue Origin. (2022, April). *New Glenn capabilities*. Retrieved 10 March 2021, from <https://www.blueorigin.com/new-glenn/>
- Borgue, O., Panarotto, M., & Isaksson, O. (2019). Modular product design for additive manufacturing of satellite components: maximising product value using genetic algorithms. *Concurrent Engineering*, 27(4), 331–346.
- Brown, W. C. (1965, December). *Experimental airborne microwave supported platform* (Contract AF30 (602) 3481 No. RADC-TR-65-188). NASA.
- Brown, W. C. (1974). The technology and application of free-space power transmission by microwave beam. *Proceedings of the IEEE*, 62(1), 11–25.
- Brown, W. C. (1977). Electronic and mechanical improvement of the receiving terminal of a free-space microwave power transmission system. *NASA STI/Recon Technical Report*, 77, 31613.
- Brown, W. C. (1980a). The history of the development of the rectenna. In *Solar power satellite microwave power transmission and reception* (p. 271).
- Brown, W. C. (1980b). Solar power satellite program rev. DOE/NASA satellite power system concept development evaluation program. In *Final proc. conf* (Vol. 800491, pp. 8–18).
- Brown, W. C. (1992). *A transportronic solution to the problem of interorbital transportation* (Tech. Rep.).
- Brown, W. C., & Eves, E. E. (1992). Beamed microwave power transmission and its application to space. *IEEE Transactions on Microwave Theory and Techniques*, 40(6), 1239–1250.
- Brown, W. C., George, R. H., Heenan, N. I., & Wonson, R. C. (1969, May 05). *Microwave to DC converter*. Google Patents. (US Patent 3434678A)
- Brown, W. C., & Triner, J. (1982). Experimental thin-film, etched-circuit rectenna. In *1982 IEEE MTT-S International Microwave Symposium Digest* (pp. 185–187).
- Cash, I. (2017). CASSIOPeia solar power satellite. In *Proc. 2017 IEEE International Conference on Wireless for Space and Extreme Environments (WiSEE)* (pp. 144–149).
- Cash, I. (2019). CASSIOPeia – a new paradigm for space solar power. *Acta Astronautica*, 159, 170–178.
- Cash, I. (2021a, 09 December). *CASSIOPeia SPS – space based solar power for net zero*. Workshop: ESA's 1st International Workshop for Space Solar Power for Net Zero.
- Cash, I. (2021b). *A phased array antenna and apparatus incorporating the same*. Intellectual Property Office UK. (UK Patent GB2563574)
- Cavalli, A., Dijkstra, A., Haverkort, J. E., & Bakkers, E. P. (2018). Nanowire polymer transfer for enhanced solar cell performance and lower cost. *Nano-Structures & Nano-Objects*, 16, 59–62.
- Chen, Q. (2020). *Research on high-performance receiving and rectifying technology for microwave wireless power transmission* (Unpublished doctoral dissertation). Sichuan University.
- Cheney, M. (1981). *Tesla, man out of time*. Englewood Cliffs, NJ, USA: Prentice-Hall.
- Clark, S. (2015, April 22). *ULA needs commercial customers to close Vulcan rocket business case*. Retrieved 25 January 2022, from <https://spaceflightnow.com/2015/04/22/ula-needs-commercial-business-to-close-vulcan-rocket-business-case/>
- Corson, D., Bradburn, N., Chodorow, M., Dougherty, J., Gordon, W., Hannon, B., ... others (1981). Electric power from orbit: A critique of a satellite power system. *National Academy of Sciences, Washington, DC*.
- Cui, Y., Duan, X., Hu, J., & Lieber, C. M. (2000). Doping and electrical transport in silicon nanowires. *The Journal of Physical Chemistry B*, 104(22), 5213–5216.
- Dallas, J., Raval, S., Gaitan, J. A., Saydam, S., & Dempster, A. (2020). The environmental impact of emissions from space launches: A comprehensive review. *Journal of Cleaner Production*, 255, 120209.
- Davis, H. P. (2012). *Space-based solar power, an update* (Tech. Rep.). Solar High Study Group.
- Dickinson, R. M. (1975). Evaluation of a microwave high-power reception-conversion array for wireless power transmission. *NASA STI/Recon Technical Report*, 76, 11207.
- Dickinson, R. M. (2003). Wireless power transmission technology state of the art – the first bill brown lecture. *Acta Astronautica*, 53(4–10), 561–570.
- Dickinson, R. M., & Brown, W. C. (1975). Radiated microwave power transmission system efficiency measurements. *NASA Tech. Memo 33-727*.
- Dickinson, R. M., & Maynard, O. (1999). Ground based wireless and wired power transmission cost comparison. *JPL TRS 1992+*.
- DoC, & NTIA. (2021, January). Manual of regulations and procedures for federal radio frequency management. *NTIA Manual*.
- Dong, Y., Dong, S.-W., Wang, Y., Liu, S., Li, X., Gao, S., ... Ran, L. (2018). Focused microwave power transmission system with high-efficiency rectifying surface. *IET Microwaves, Antennas & Propagation*, 12(5), 808–813.
- Espinet-Gonzalez, P., Barrigón, E., Chen, Y., Otnes, G., Vescovi, G., Mann, C., ... others (2020). Nanowire solar cells: a new radiation hard PV technology for space applications. *IEEE Journal of Photovoltaics*, 10(2), 502–507.
- Espinet-Gonzalez, P., Barrigón, E., Otnes, G., Vescovi, G., Mann, C., France, R. M., ... others (2019). Radiation tolerant nanowire array solar cells. *ACS Nano*, 13(11), 12860–12869.
- Etani, S., Iwashita, M., & Kaya, N. (2011). Development on the sandwich panel for the practical solar power satellite. In *Proc. of the 28th international symposium on space technology and science*.
- Euroconsult. (2021, December). *Satellites to be built and launched by 2030* (No. 24).
- Foust, J. (2008, 15 September). A step forward for space solar power. *The Space Review*. Retrieved 13 April 2022, from <https://www.thespacereview.com/article/1210/1>
- Fujino, Y., et al. (1993, February). A rectenna for MILAX. In *Proc. wireless power transmissions conference* (pp. 273–277).
- Gal-Katziri, M., Fikes, A., Bohn, F., Abiri, B., Hashemi, M. R., & Hajimiri, A. (2020). Scalable, deployable, flexible phased array sheets. In *Proc. 2020 IEEE/MTT-S international microwave symposium (IMS)* (pp. 1085–1088).
- Gal-Katziri, M., & Hajimiri, A. (2018). A sub-picosecond hybrid dll for large-scale phased array synchronization. In *2018 IEEE Asian solid-state circuits conference (A-SSCC)* (pp. 231–234).
- Gal-Katziri, M., Ives, C., Khakpour, A., & Hajimiri, A. (2022). Optically synchronized phased arrays in CMOS. *IEEE Journal of Solid-State Circuits*.
- Garcia, M. (2021, November 4). *International space station facts and figures*. NASA. Retrieved 09 January 2022, from <https://www.nasa.gov/feature/facts-and-figures>
- Gdoutos, E., Leclerc, C., Royer, F., Türk, D. A., & Pellegrino, S. (2019). Ultralight spacecraft structure prototype. In *AIAA Scitech 2019 Forum* (p. 1749).
- Gdoutos, E., Truong, A., Pedivellano, A., Royer, F., & Pellegrino, S. (2020). Ultralight deployable space structure prototype. In *AIAA Scitech 2020 Forum* (p. 0692).
- George, R., & Okress, E. (1968). Solid state power rectifications. *Microwave power engineering*, 1, 275–294.
- Gibb, J. (2018). Lightweight flexible space solar arrays, past, present and future. In *2018 IEEE 7th world conference on photovoltaic energy conversion (WCPEC) (A joint conference of 45th IEEE PVSC, 28th PVSEC 34th EU PVSEC)* (p. 3530–3534).
- Glaser, P. (1968). Power from the sun: Its future. *Science*, 162(3856), 857–861.
- Glaser, P. (1973, December 25). *Method and apparatus for converting solar radiation to electrical power*. Google Patents. (US Patent 3,781,647)
- Goel, A., Chung, S.-J., & Pellegrino, S. (2017, June). Trajectory design of a spacecraft formation for space-based solar power using sequential convex programming. In *Proc. conference 9th international workshop on satellite constellations and formation flying (IWSCFF)*.

- Goel, A., Lee, N., & Pellegrino, S. (2017). Trajectory design of formation flying constellation for space-based solar power. In *2017 IEEE aerospace conference* (pp. 1–11).
- Grandidier, J., Jaffe, P., Roberts, W. T., Wright, M. W., Fraeman, A. A., Raymond, C. A., ... others (2021). Laser power beaming for lunar night and permanently shadowed regions. *Jet Propulsion*, 818, 354–1566.
- Grebennikov, A. (2011). *RF and microwave transmitter design* (Vol. 234). John Wiley & Sons.
- Greenfieldboyce, N. (2021, December 22). *Why some astronomers once feared NASA's James Webb space telescope would never launch*. Retrieved 04 April 2022, from <https://n.pr/3vgyenz>
- Hagerty, J. A., & Popovic, Z. (2001). An experimental and theoretical characterization of a broadband arbitrarily-polarized rectenna array. In *2001 IEEE MTT-S international microwave symposium digest (Cat. No. 01CH37157)* (Vol. 3, pp. 1855–1858).
- Hajimiri, A., Abiri, B., Bohn, F., Gal-Katziri, M., & Manohara, M. H. (2020). Dynamic focusing of large arrays for wireless power transfer and beyond. *IEEE Journal of Solid-State Circuits*.
- Hajimiri, S. A., Atwater, H. A., Pellegrino, S., Abiri, B., & Bohn, F. (2021). *Large-scale space-based solar power station: power transmission using steerable beams*. Google Patents. (US Patent 11,128,179)
- Hashemi, M. R. M., Fikes, A. C., Gal-Katziri, M., Abiri, B., Bohn, F., Saifipour, A., ... others (2019). A flexible phased array system with low areal mass density. *Nature Electronics*, 2(5), 195–205.
- Hawkins, J., Houston, S., Hatfield, M., & Brown, W. (1998). The saber microwave-powered helicopter project and related wpt research at the University of Alaska Fairbanks. In *AIP conference proceedings* (Vol. 420, pp. 1092–1097).
- Heinzler, R., Schindler, P., Seekircher, J., Ritter, W., & Stork, W. (2019). Weather influence and classification with automotive lidar sensors. In *2019 IEEE intelligent vehicles symposium (IV)* (pp. 1527–1534).
- Hou, X., & Li, M. (2021, 09 December). *Activities of SPS development in China*. Workshop: ESA's 1st International Workshop for Space Solar Power for Net Zero.
- Hu, L., Zhao, Q., Huang, S., Zheng, J., Guan, X., Patterson, R., ... others (2021). Flexible and efficient perovskite quantum dot solar cells via hybrid interfacial architecture. *Nature Communications*, 12(1), 1–9.
- IEA. (2020). *World energy outlook 2020*. OECD Publishing.
- IEEE Standards Coordinating Committee. (2019, October). *IEEE standard for safety levels with respect to human exposure to radio frequency electromagnetic fields, 3kHz to 300GHz* (Tech. Rep. No. IEEE Std C95.1-2019).
- IPCC. (2022, April). *AR6 Synthesis Report: Climate Change 2022*. Retrieved 10 April 2022, from <https://www.ipcc.ch/assessment-report/ar6/>
- ITU. (2019, August). *Attenuation due to clouds and fog* (Standard No. ITU-R P840). International Telecommunication Union (ITU).
- ITU. (2021a, 06). *Applications of wireless power transmission via radio frequency beam* (Tech. Rep. No. ITU-R SM.2392-1). International Telecommunication Union (ITU).
- ITU. (2021b, October). *ITU-R: Managing the radio-frequency spectrum for the world*. Retrieved 25 January 2022, from <https://www.itu.int/en/mediacentre/backgrounders/Pages/itu-r-managing-the-radio-frequency-spectrum-for-the-world.aspx>
- Jaffe, P. (2013). *A sunlight to microwave power transmission module prototype for space solar power* (Unpublished doctoral dissertation). University of Maryland, College Park.
- Jaffe, P. (2020). 24 - Space Solar. In T. M. Letcher (Ed.), *Future energy* (Third ed., p. 519-542). Elsevier.
- Jehn, R., Agapov, V., & Hernández, C. (2005). The situation in the geostationary ring. *Advances in space research*, 35(7), 1318–1327.
- Jones, H. (2018, July). The recent large reduction in space launch cost. In *Proc. 48th international conference on environmental systems*.
- Kalyuzhnyy, N. A., Emelyanov, V. M., Evstropov, V. V., Mintairov, S. A., Mintairov, M. A., Nahimovich, M. V., ... Shvarts, M. Z. (2020). Optimization of photoelectric parameters of InGaAs metamorphic laser ( $\lambda = 1064$  nm) power converters with over 50% efficiency. *Solar Energy Materials and Solar Cells*, 217, 110710.
- Kang, S., Jeong, J., Cho, S., Yoon, Y. J., Park, S., Lim, S., ... Ko, H. (2019). Ultrathin, lightweight and flexible perovskite solar cells with an excellent power-per-weight performance. *Journal of Materials Chemistry A*, 7(3), 1107–1114.
- Kawashima, N., & Takeda, K. (2004). 1.2 km laser energy transmission for the development of a lunar rover confirming the presence of ice on the moon (AAS 03-737). In *International lunar conference 2003* (Vol. 108, p. 291).
- Kawashima, N., & Takeda, K. (2008). Laser energy transmission for a wireless energy supply to robots. *Robotics and Automation in Construction*, 10, 373–380.
- Kaya, N. (1996). Transmitting antenna system for airship demonstration (ETHER). *Space Energy and Transportation*, 1(4), 237–245.
- Kaya, N., Kojima, H., Matsumoto, H., Hinada, M., & Akiba, R. (1994). ISY-METS rocket experiment for microwave energy transmission. *Acta Astronautica*, 34, 43-46.
- Kayes, B. M., Zhang, L., Twist, R., Ding, I.-K., & Higashi, G. S. (2014). Flexible thin-film tandem solar cells with gt;30efficiency. *IEEE Journal of Photovoltaics*, 4(2), 729-733.
- Kazmierski, T. J., & Beeby, S. (2014). *Energy harvesting systems*. Springer.
- Kelzenberg, M. D., Espinet-Gonzalez, P., Vaidya, N., Warmann, E. C., Naqavi, A., Loke, S. P., ... others (2018). Ultralight energy converter tile for the space solar power initiative. In *2018 IEEE 7th world conference on photovoltaic energy conversion (WCPEC)(A Joint Conference of 45th IEEE PVSEC, 28th PVSEC & 34th EU PVSEC)* (pp. 3357–3359).
- Kim, N.-K., Min, Y. H., Noh, S., Cho, E., Jeong, G., Joo, M., ... others (2017). Investigation of thermally induced degradation in CH<sub>3</sub>NH<sub>3</sub>PbI<sub>3</sub> perovskite solar cells using in-situ synchrotron radiation analysis. *Scientific reports*, 7(1), 1–9.
- Koblin, W., Krüger, E., & Schuh, U. (1984). *Handbuch Passive Nutzung der Sonnenenergie*. Bonn: Ministerium für Raumordnung, Bauwesen und Städtebau.
- Koomanoff, F. A. (1981). Satellite power system concept development and evaluation program. *Space Sol. Power Rev.* (CONF-800672-2).
- Lang, F., Nickel, N. H., Bundesmann, J., Seidel, S., Denker, A., Albrecht, S., ... others (2016). Radiation hardness and self-healing of perovskite solar cells. *Advanced Materials*, 28(39), 8726–8731.
- Larson, W. J., & Wertz, J. R. (1992). *Space mission analysis and design* (Tech. Rep.). Torrance, CA (United States); Microcosm, Inc.
- Law, D. C., Edmondson, K., Siddiqi, N., Paredes, A., King, R., Glenn, G., ... Karam, N. (2006). Lightweight, flexible, high-efficiency III-V multijunction cells. In *2006 IEEE 4th world conference on photovoltaic energy conference* (Vol. 2, p. 1879-1882).
- Lei, Z. (2019, 27 February). *Scientists envision solar power station in space*. Retrieved 04 March 2022, from <http://www.chinadaily.com.cn/a/201902/27/WS5c75c8b3a3106c65c34eb8e3.html>
- Letier, P., Yan, X. T., Deremetz, M., Bianco, A., Grunwald, G., Roa, M., ... others (2019). MOSAR: Modular spacecraft assembly and reconfiguration demonstrator. In *Proc. 15th symposium on advanced space technologies in robotics and automation*.
- Ludin, N. A., Mustafa, N. I., Hanafiah, M. M., Ibrahim, M. A., Teridi, M. A. M., Sepeai, S., ... Sopian, K. (2018). Prospects of life cycle assessment of renewable energy from solar photovoltaic technologies: a review. *Renewable and Sustainable Energy Reviews*, 96, 11–28.
- Madonna, R. G. (2018). Use of an iterative research and development-system engineering approach for the caltech space solar power project. In *Proc. 2018 6th IEEE international conference on wireless for space and extreme environments (WiSEE)* (pp. 200–205).
- Madonna, R. G. (2021, 09 December). *Caltech space solar power project*. Workshop: ESA's 1st International Workshop for Space Solar Power for Net Zero.
- Malinkiewicz, O., Imaizumi, M., Sapkota, S. B., Ohshima, T., & Öz, S. (2020). Radiation effects on the performance of flexible perovskite solar cells for space applications. *Emergent Materials*, 3(1), 9–14.
- Mankins, J. (1997). A fresh look at space solar power: New architectures, concepts and technologies. *Acta Astronautica*, 41(4-10), 347–359.
- Mankins, J. (2017). New developments in space solar power. *NSS Space Settlement Journal*, 1–30.
- Mankins, J. (2021, 09 December). *SPS-ALPHA and the economics of space solar power*. Workshop: ESA's 1st International Workshop for Space Solar Power for Net Zero.
- Mankins, J., Kaya, N., & Vasile, M. (2012). SPS-ALPHA: The first practical solar power satellite via arbitrarily large phased array (a 2011-2012 NIAC project). In *Proc. 10th international energy conversion engineer-*

- ing conference (p. 3978).
- Marshall, M. A., Goel, A., & Pellegrino, S. (2020). Power-optimal guidance for planar space solar power satellites. *Journal of Guidance, Control, and Dynamics*, 43(3), 518–535.
- Marshall, M. A., Madonna, R. G., & Pellegrino, S. (2021). Investigation of equatorial medium earth orbits for space solar power. *IEEE Transactions on Aerospace and Electronic Systems*.
- Masrur, M. A., & Cox, M. (2019). A unique military application of wireless power transfer: Wireless charging through a vehicle seat with simplified design considerations. *IEEE Industrial Electronics Magazine*, 13(4), 19–30.
- Matsumoto, H. (1989). Microwave energy transmission. *Nippon Koku Uchu Gakkaishi (Japan)*, 37(422).
- Matsumoto, H. (2002). Research on solar power satellites and microwave power transmission in Japan. *IEEE microwave magazine*, 3(4), 36–45.
- Matsumoto, H., Kaya, N., Kimura, I., Miyatake, S., Nagatomo, M., & Obayashi, T. (1982). MINIX project toward the solar power satellite-rocket experiment of microwave energy transmission and associated nonlinear plasma physics in the ionosphere. In *Proc. ISAS space energy symposium* (pp. 69–76).
- Maynard, O. E., & Blick, E. F. (1980). *Solid state SPS microwave generation and transmission study* (Vol. 3338). NASA.
- McSpadden, J. O., & Mankins, J. C. (2002). Space solar power programs and microwave wireless power transmission technology. *IEEE microwave magazine*, 3(4), 46–57.
- Mihara, S., Maekawa, K., Nakamura, S., Sasaki, K., Homma, Y., Hangai, M., ... others (2018). The plan of microwave power transmission development for SSPS and its industry application. In *Proc. 2018 asia-pacific microwave conference (APMC)* (pp. 443–445).
- Mihara, S., Sato, M., Nakamura, S., Sasaki, K., Homma, Y., Sasaki, T., ... Fujiwara, T. (2015). The result of ground experiment of microwave wireless power transmission. In *Proc. 66th international astronautic congress*.
- Miyazawa, Y., Ikegami, M., Chen, H.-W., Ohshima, T., Imaizumi, M., Hirose, K., & Miyasaka, T. (2018). Tolerance of perovskite solar cell to high-energy particle irradiations in space environment. *iScience*, 2, 148–155.
- Mizojiri, S., Takagi, K., Shimamura, K., Yokota, S., Fukunari, M., Tatematsu, Y., & Saito, T. (2019). Demonstration of sub-terahertz coplanar rectenna using 265 GHz gyrotron. In *Proc. 2019 IEEE wireless power transfer conference (WPTC)* (pp. 409–412).
- NASA. (1978, October). *Satellite power system concept development and evaluation program, reference system report* (Tech. Rep. No. Rep. DOE/ER-0023). Department of Energy.
- Needell, D. R., Bauser, H., Phelan, M., Bukowsky, C. R., Ilic, O., Kelzenberg, M. D., & Atwater, H. A. (2019). Ultralight luminescent solar concentrators for space solar power systems. In *Proc. 2019 IEEE 46th photovoltaic specialists conference (PVSC)* (pp. 2798–2801).
- Needell, D. R., Ilic, O., Bukowsky, C. R., Nett, Z., Xu, L., He, J., ... others (2018). Design criteria for micro-optical tandem luminescent solar concentrators. *IEEE Journal of Photovoltaics*, 8(6), 1560–1567.
- Needell, D. R., Nett, Z., Ilic, O., Bukowsky, C. R., He, J., Xu, L., ... others (2017). Micro-optical tandem luminescent solar concentrator. In *Proc. 2017 IEEE 44th photovoltaic specialist conference (PVSC)* (pp. 1737–1740).
- Nishioka, T., & Yano, S. (2015, 16 March). *Mitsubishi heavy takes step toward long-distance wireless power*. Retrieved 20 December 2021, from <https://asia.nikkei.com/Business/Biotechnology/Mitsubishi-Heavy-takes-step-toward-long-distance-wireless-power>
- NRL. (2019, October). *Press release: Researchers transmit energy with laser in 'historic' power-beaming demonstration*. Retrieved 13 February 2022, from <https://bit.ly/37M5QBw>
- NRL. (2020, 18 May). *Press release: Nrl conducts first test of solar power satellite hardware in orbit*. Retrieved 13 February 2022, from <https://bit.ly/3vfPIR4>
- Nugent, T., Bashford, D., Bashford, T., Sayles, T., & Hay, A. (2020). Long-range integrated safe laser power beaming demonstration. In *Proc. optical wireless fiber power transmission conference (OWPT)* (pp. 12–13).
- O'Quinn, C., & Jones, K. (2022). Increased access to space with modularity and interface standards. In *AIAA Scitech 2022 forum* (p. 647).
- Park, Y., Kim, K., & Youn, D. (2018). Rectenna array design for receiving high power in beam type wireless power transmission. In *Proc. 2018 Asia-Pacific microwave conference (APMC)* (pp. 440–442).
- Pedivellano, A., Gdoutos, E., & Pellegrino, S. (2020). Sequentially controlled dynamic deployment of ultra-thin shell structures. In *AIAA Scitech 2020 forum*. American Institute of Aeronautics and Astronautics.
- Pellegrino, S., Atwater, H. A., Hajimiri, S. A., Gdoutos, E. E., Leclerc, C., Royer, F. A., & Pedivellano, A. (2020, January 23). *Coilable thin-walled longerons and coilable structures implementing longerons and methods for their manufacture and coiling*. Google Patents. (US Patent App. 16/514,793)
- Penn, J., Law, G., et al. (2001). The aerospace corporation systems studies and analysis of the space solar power (SSP) exploratory research and technologies concepts and applications. *Aerospace Report No. ATR-01 (7710)-1*, 9, 106.
- Philipps, S. P., Dimroth, F., & Bett, A. W. (2018). High-efficiency III–V multi-junction solar cells. In *McEvoy's handbook of photovoltaics* (pp. 439–472). Elsevier.
- Pisacane, V. L. (2005). *Fundamentals of space systems*. Johns Hopkins University Applied Physics Laboratory Series in Science and Engineering.
- Potter, P. D. (1961). A new horn antenna with suppressed sidelobes and equal beam widths. *Microwave journal*, 6(6), 71–78.
- Qiu, H., Liu, H., Jia, X., Jiang, Z.-Y., Liu, Y.-H., Xu, J., ... Chen, K. J. (2021). Compact, flexible, and transparent antennas based on embedded metallic mesh for wearable devices in 5G wireless network. *IEEE Transactions on Antennas and Propagation*, 69(4), 1864–1873.
- Roberts, T. (2020, 02 September). *Space launch to low earth orbit: How much does it cost?* Retrieved 26 March 2022, from <https://bit.ly/3rojZMv>
- Rodenbeck, C. T., Jaffe, P. I., Strassner II, B. H., Hausgen, P. E., McSpadden, J. O., Kazemi, H., ... Self, A. P. (2021). Microwave and millimeter wave power beaming. *IEEE Journal of Microwaves*, 1(1), 229–259.
- Rodenbeck, C. T., Tierney, B. B., Park, J., Parent, M. G., DePuma, C. B., Bauder, C. J., ... Mayhan, T. (2022). Terrestrial microwave power beaming. *IEEE Journal of Microwaves*.
- Rogers, J. E., & Spirnak, G. T. (2005, August 30). *Space-based power system*. Google Patents. (US Patent 6,936,760)
- Roulette, J. (2022, February 11). *What is Starship? SpaceX builds its next-generation rocket*. Retrieved 13 April 2022, from <https://www.nytimes.com/article/elon-musk-starship.html>
- Rubenchik, A., Parker, J., Beach, R., & Yamamoto, R. (2009). *Solar power beaming: From space to earth* (Tech. Rep.). Lawrence Livermore National Lab.(LLNL), Livermore, CA (United States).
- Saad, W., Bennis, M., & Chen, M. (2019). A vision of 6G wireless systems: Applications, trends, technologies, and open research problems. *IEEE Network*, 34(3), 134–142.
- Sasaki, S., Tanaka, K., & Maki, K. (2013). Microwave power transmission technologies for solar power satellites. *Proceedings of the IEEE*, 101(6), 1438–1447.
- Schlesak, J., Alden, A., & Ohno, T. (1985, December). SHARP rectenna and low altitude flight trials. In *IEEE global telecommunications conference*.
- SDSC. (2016, 03 April). *Press release: Space solar power dominates the D3*. Retrieved 03 December 2021, from <https://bit.ly/3EfCvM3>
- Shaulov, E., Jameson, S., & Socher, E. (2017). W-band energy harvesting rectenna array in 65-nm CMOS. In *Proc. 2017 IEEE MTT-S international microwave symposium (IMS)* (pp. 307–310).
- Shinohara, N. (2013). Beam control technologies with a high-efficiency phased array for microwave power transmission in Japan. *Proceedings of the IEEE*, 101(6), 1448–1463.
- Shinohara, N. (2014). *Wireless power transfer via radiowaves*. John Wiley & Sons.
- Shinohara, N., Hasegawa, N., Kojima, S., & Takabayashi, N. (2019). New beam forming technology for narrow beam microwave power transfer. In *Proc. 8th Asia-Pacific conference antennas propagation (AP-CAP)*.
- Shinohara, N., & Matsumoto, H. (1998). Dependence of DC output of a rectenna array on the method of interconnection of its array elements

- output of a rectenna array on the method of interconnection of its array elements. *Electrical Engineering in Japan*, 125(1), 9–17.
- Shinohara, N., Matsumoto, H., & Hashimoto, K. (2004). Phase-controlled magnetron development for sports: Space power radio transmission system. *URSI Radio Science Bulletin*, 2004(310), 29–35.
- Silva, Z. J., Valenta, C. R., & Durgin, G. D. (2020). Optically transparent antennas: A survey of transparent microwave conductor performance and applications. *IEEE Antennas and Propagation Magazine*, 63(1), 27–39.
- Skowron, J., MacMaster, G., & Brown, W. (1964). The super power CW amplatron. *Microwave Journal*, 7.
- Solarex. (2022). *About us: Our businesses*. Retrieved 11 February 2022, from <https://www.solarexspace.com/our-company/our-businesses/>
- Song, K. D., Kim, J., Kim, J. W., Park, Y., Ely, J. J., Kim, H. J., & Choi, S. H. (2019). Preliminary operational aspects of microwave-powered airship drone. *International Journal of Micro Air Vehicles*, 11.
- SpaceX. (2020, March). *Starship users guide*. Retrieved 02 April 2022, from [https://www.spacex.com/media/starship\\_users\\_guide\\_v1.pdf](https://www.spacex.com/media/starship_users_guide_v1.pdf)
- SpaceX. (2021, September). *Rideshare payload user's guide*. Retrieved 02 April 2022, from [https://storage.googleapis.com/rideshare-static/Rideshare\\_Payload\\_Users\\_Guide.pdf](https://storage.googleapis.com/rideshare-static/Rideshare_Payload_Users_Guide.pdf)
- SpaceX. (2022). *Capabilities & services*. Retrieved 02 April 2022, from <https://www.spacex.com/media/Capabilities&Services.pdf>
- Strassner, B., & Chang, K. (2003a). 5.8-GHz circularly polarized dual-rhombic-loop traveling-wave rectifying antenna for low power density wireless power transmission applications. *IEEE Transactions on Microwave Theory and Techniques*, 51(5), 1548–1553.
- Strassner, B., & Chang, K. (2003b). Highly efficient C-band circularly polarized rectifying antenna array for wireless microwave power transmission. *IEEE Transactions on Antennas and Propagation*, 51(6), 1347–1356.
- Stutzman, W. L., & Thiele, G. A. (2012). *Antenna theory and design* (3rd ed.). New York: Wiley.
- Summerer, L., & Ongaro, F. (2005). Advanced space technology for 21st century energy systems: Solar power from space. In *Proc. 2005 2nd international conference on recent advances in space technologies, (RAST)* (pp. 16–23).
- Summerer, L., & Purcell, O. (2009). Concepts for wireless energy transmission via laser. *European Space Agency (ESA)-Advanced Concepts Team*.
- Takahashi, T., Sasaki, T., Homma, Y., Mihara, S., Sasaki, K., Nakamura, S., ... Ohashi, K. (2016). Phased array system for high efficiency and high accuracy microwave power transmission. In *Proc. 2016 IEEE international symposium on phased array systems and technology (PAST)* (pp. 1–7).
- Tanaka, K. (2021, 09 December). *Efforts to develop solar power satellite in Japan over the past 10 years*. Workshop: ESA's 1st International Workshop for Space Solar Power for Net Zero.
- Tao, H., Su-Hui, Y., Munoz, M. A., Hai-Yang, Z., Chang-Ming, Z., Yi-Chen, Z., & Peng, X. (2014). High-power high-efficiency laser power transmission at 100 m using optimized multi-cell GaAs converter. *Chinese Physics Letters*, 31(10), 104203.
- Tesla, N. (1904). The transmission of electrical energy without wires. *Electrical World and Engineer*, 1, 21–24.
- The Economist. (2021a, 25 February). Electricity can be transmitted through the air. *The Economist*. Retrieved from <https://www.economist.com/science-and-technology/2021/02/25/electricity-can-be-transmitted-through-the-air>
- The Economist. (2021b, 20 November). *A russian anti-satellite missile test puts the iss in peril*. Retrieved 22 November 2022, from <https://www.economist.com/science-and-technology/2021/11/18/a-russian-anti-satellite-missile-test-puts-the-iss-in-peril>
- The Laser Institute. (2014). *Safe use of lasers* (No. ANSI Z136.1).
- Turpin, T. W., & Baktur, R. (2009). Meshed patch antennas integrated on solar cells. *IEEE Antennas and Wireless Propagation Letters*, 8, 693–696.
- URSI. (2007, June). *URSI white paper on solar power satellite (SPS) systems and report of the URSI inter-commission working group on SPS*. Retrieved from <https://www.ursi.org/files/ICWGRReport070611.pdf>
- Warmann, E. C., Espinet-Gonzalez, P., Vaidya, N., Loke, S., Naqavi, A., Vinogradova, T., ... others (2020). An ultralight concentrator photovoltaic system for space solar power harvesting. *Acta Astronautica*, 170, 443–451.
- Way, S., & Lamyman, J. (2020, December). *Space based solar power as a contributor to net zero - phase 1: Engineering feasibility report* (Tech. Rep.). Frazer-Nash Consultancy.
- Way, S., & Lamyman, J. (2021a, April). *Space based solar power as a contributor to net zero - phase 2: Economic feasibility* (Tech. Rep.). Frazer-Nash Consultancy.
- Way, S., & Lamyman, J. (2021b, September). *Space based solar power: De-risking the pathway to net zero* (Tech. Rep.). Frazer-Nash Consultancy.
- Wilson, A. R. (2019). *Advanced methods of life cycle assessment for space systems* (Unpublished doctoral dissertation). University of Strathclyde.
- Xu, Y., Li, J., Tan, Q., Peters, A. L., & Yang, C. (2018). Global status of recycling waste solar panels: A review. *Waste Management*, 75, 450–458.
- Yeary, M., Palmer, R., Fulton, C., Salazar, J., & Sigmarsson, H. (2021). Update on an S-band all-digital mobile phased array radar. In *Proc. 2021 IEEE radar conference* (pp. 1–4).
- York, M. C., & Fafard, S. (2017). High efficiency phototransducers based on a novel vertical epitaxial heterostructure architecture (VEHSA) with thin p/n junctions. *Journal of Physics D: Applied Physics*, 50(17), 173003.
- Zhang, B., Jiang, W., Yang, Y., Yu, C., Huang, K., & Liu, C. (2015). Experimental study on an S-band near-field microwave magnetron power transmission system on hundred-Watt level. *International Journal of Electronics*, 102(11), 1818–1830.
- Zhang, H., & Liu, C. (2016). A high-efficiency microwave rectenna array based on subarray decomposition. *Applied Science Technology*, 10(4), 57–61.
- Zhang, L.-C., & Shi, L.-X. (2022). Design of 70% PAE class-F 1.2–1.4 GHz 10 W GaN power amplifier MMIC. *Microwave and Optical Technology Letters*, 64(4), 670–675.